

An Adaptive Hybrid Control Algorithm for Sender-Receiver Clock Synchronization

Marcello Guarro
mguarro@ucsc.edu
Ricardo Sanfelice
ricardo@ucsc.edu

October 20, 2022

Technical Report
Hybrid Systems Laboratory
Department of Computer Engineering
University of California, Santa Cruz

Technical Report No. TR-HSL-01-2020

Available at <https://hybrid.soe.ucsc.edu/biblio>

Readers of this material have the responsibility to inform all of the authors promptly if they wish to reuse, modify, correct, publish, or distribute any portion of this report.

An Adaptive Hybrid Control Algorithm for Sender-Receiver Clock Synchronization

October 20, 2022

Abstract

This paper presents an innovative hybrid systems approach to the sender-receiver synchronization of timers. Via the hybrid systems framework, we unite the traditional sender-receiver algorithm for clock synchronization with an online, adaptive strategy to achieve synchronization of the clock rates to exponentially synchronize a pair of clocks connected over a network. Following the conventions of the algorithm, clock measurements of the nodes are given at periodic time instants, and each node uses these measurements to achieve synchronization. For this purpose, we introduce a hybrid system model of a network with continuous and impulsive dynamics that captures the sender-receiver algorithm as a state-feedback controller to synchronize the network clocks. Moreover, we provide sufficient design conditions that ensure attractivity of the synchronization set.

1 Introduction

1.1 Motivation

The consensus on a common timescale in a distributed system is an essential requisite for any coordinated system whose algorithm or task depends on the event-ordering of its input. Moreover, distributed algorithms that interact with a dynamical system have the additional requirement of having to know the precise moment an event occurs to ensure desired system function, stability, and safety. This has become increasingly apparent in the deployment of large and complex cyber-physical systems such as autonomous vehicles [1], aerospace avionics, and distributed manufacturing robotic systems [2].

It has been well established in the literature on networked control systems, that the lack of consensus on a shared timescale among distributed agents can result in performance issues that adversely affect system stability, see [3] and [4]. In particular, time delays due to sampling, transmission, and computation result in the loss of concurrency between the dynamic process events of the plant and computational process events of the system planner or controller (see [5]). To address this issue, system events are time-stamped via clocks local to the sensors and actuators that interact with the physical systems as noted in [5] and the survey papers [4], [6]. However, the success of this strategy relies on the existence of a common timescale among the components and agents in the distributed system. To ensure consensus on a common timescale, the system is coupled with a clock synchronization subsystem that periodically synchronizes the clocks to ensure their relative error is within an acceptable tolerance that is sufficient for desired system performance.

The design of such a subsystem, however, is nontrivial as network delays, nonuniform clock drifts, and the lack of an absolute time reference, present a unique set of challenges to the clock synchronization problem as noted in [7], [8], and [9]. Network delays, such as those due to computation or transmission processes, are often the key challenge in synchronization due to the inherent difficulty of their estimation. Of particular concern, however, is the influence of the clock synchronization subsystem on ensuring the stability and robustness guarantees of the larger system as observed in [3] and [10]. In [11], we demonstrate a sufficient finite-time convergence condition on the clock synchronization subsystem in a time-stamp aware observer to ensure asymptotic convergence of the estimation error.

In this paper, we are interested in designing a clock synchronization algorithm using two-way communication protocols with tractable design conditions and performance metrics to meet the current and projected demands of distributed system design. In particular, we are interested in the design of algorithm that addresses the following challenges:

- *Communication delays*: the physical nature and operation of communication networks introduces a variety of stochastic and deterministic delays that adversely affect accurate synchronization of time. As previously noted, two primary sources of communication delay are those that relate to transmission and computation (also known as residence delay).
- *Clocks with different rates of change*: typical clocks deployed in a distributed system are inherently imprecise devices whose frequency or

clock rate is subjected to noise disturbances due to physical, environmental, and manufacturing constraints.

- *Performance guarantees:* noting the influence of delays on networked control systems and the time-stamping approach used to alleviate them, guarantees on the synchronization performance are necessary when the control system is subjected to fast sampling periods, as noted in [12].

1.2 Related Work

Among the number of existing algorithms for clock synchronization, sender-receiver (or two-way) based synchronization algorithm underpin several of the most popular clock synchronization protocols including Network Time Protocol (NTP) in [13] , Precision Time Protocol (PTP) in [14] , and the Timing-sync Protocol for Sensor Networks (TPSN) in [15].

The core algorithm, upon which these protocols are based, relies on the existence of a known reference that is either injected to the system or provided by an elected agent in the distributed system; synchronization is then achieved through a series of chronologically ordered and time stamped two-way message exchanges between each synchronizing node and the designated reference. With sufficient information from the exchanged messages and underlying assumptions on the clocks and communication delays, the relative differences in the clock rates and offset can be estimated and applied as a correction to the clock of the synchronizing node, see [16]. However, while the difference in the output can be determined and implemented online, the relative clock rate is estimated through offline filtering techniques (see [13]) or least-squares estimation (see [7]).

Each of the aforementioned protocols, however, utilize different strategies in regards to the availability of the algorithm and the layer of implementation. For instance, the Network Time Protocol is an “always-on” implementation that runs entirely as a system process in the software layer. This level of implementation subjects the protocol to frequent computational delays due to the execution of system processes that have higher priority. These delays contribute to timing inaccuracy that renders NTP unfit for networked control systems with fast sampling periods, see [12].

Improving upon NTP to address its concerns and meet the demands of time-sensitive distributed system, the Precision Time Protocol utilizes a hybrid implementation of software and hardware to improve the synchronization accuracy. The protocol utilizes time-stamping of the exchanged

messages at the hardware layer to minimize the computational delays associated with software time-stamps on the exchanged messages.

The Timing-sync Protocol for Sensor Networks seeks to address the scalability issues posed by the NTP and PTP protocols by allowing the algorithm to work on an intermittent schedule. The intermittent strategy enable its use in low-energy sensor networks with limited computational capacity at the cost of synchronization accuracy.

Finally, while there are more recent consensus-based synchronization algorithms such as [17], [18], [19], [20], and the authors own [21], we would like to emphasize that the scope of this work is specific to synchronization algorithms that operate via a sender-receiver-based messaging protocol. Most consensus-based algorithms assume asymmetric communication protocols with one-way messaging between any two agents.

1.3 Contributions and Organization

In this paper, we present a hybrid systems approach to sender-receiver synchronization with an, online, adaptive method to synchronize the clock rates. We show that our algorithm exponentially synchronizes a pair of clocks connected over a network while preserving the messaging protocols and network dynamics of traditional sender-receiver algorithms.

Our proposed solution provides a Lyapunov-based convergence analysis to a set in which the clocks are synchronized with sufficient conditions ensuring their synchronization. In particular the main contributions of this paper are given as follows:

- In Section 4, a hybrid system model of the sender-receiver synchronization algorithm using the framework proposed in [22] is presented. The proposed model captures the continuous dynamics of the clock states and the hybrid dynamics of the networking protocol by which the timing messages are exchanged for a pair of system nodes to achieve synchronization.
- In Section 4.3, we show, through the satisfaction of some basic conditions on the system model, that the algorithm is finite-time attractive to a forward invariant set of interest that represents the correct initialization of the algorithm.
- In Section 5, we provide sufficient conditions on the algorithm parameters to show asymptotic attractivity of the hybrid system to a

set of interest representing synchronization of the clocks from the initialization set. Furthermore, we characterize the bound for solution trajectories to the systems in terms of parameters that can be used for algorithm design.

- In Section 6, we present a multi-agent extension of the proposed model to cover the case of synchronizing the nodes on an n -node network. The feasibility of this multi-agent model is validated with a numerical example of the simulated system.

Unlike the existing algorithms of NTP, PTP, and TPSN, we emphasize to the reader that previous analyses on sender-receiver synchronization have only provided results to their feasibility and that the literature lacks formal results that characterize its performance in a dynamical system setting.

In addition to the highlighted sections, this paper is organized as follows: Section 2.1 introduces the sender-receiver algorithm as presented in the literature. Section 2 outlines the motivation for this paper. Section 3 presents some preliminary material on hybrid systems. Section 4 formally introduces the problem under consideration and the hybrid model that solves it. Section 5 details the main results, while Section 7 provides numerical examples.

We inform the reader that this work is an extension of our preliminary conference paper [23]. In particular, we include the full proofs of the main results in addition to incremental results and their associated proofs that were originally omitted from the preliminary paper. Moreover, the proofs and material in Section 5 are new. In addition, new examples for the nominal and multi-agent setting are presented in Section 7.

Notation: In this paper the following notation and definitions will be used. The set of natural numbers including zero, i.e., $\{0, 1, 2, \dots\}$ is denoted by \mathbb{N} . The set of natural numbers is denoted as $\mathbb{N}_{>0}$, i.e., $\mathbb{N}_{>0} = \{1, 2, \dots\}$. The set of real numbers is denoted as \mathbb{R} . The set of non-negative real numbers is denoted by $\mathbb{R}_{\geq 0}$, i.e., $\mathbb{R}_{\geq 0} = [0, \infty)$. The n -dimensional Euclidean space is denoted \mathbb{R}^n . Given topological spaces A and B , $F : A \rightrightarrows B$ denotes a set-valued map from A to B . For a matrix $A \in \mathbb{R}^{n \times m}$, A^\top denotes the transpose of A . Given a vector $x \in \mathbb{R}^n$, $|x|$ denotes the Euclidean norm. Given two vectors $x \in \mathbb{R}^n$ and $y \in \mathbb{R}^m$, $(x, y) = [x^\top \ y^\top]^\top$. For two symmetric matrices $A \in \mathbb{R}^{n \times m}$ and $B \in \mathbb{R}^{n \times m}$, $A \succ B$ means that $A - B$ is positive definite, conversely $A \prec B$ means that $A - B$ is negative definite. Given a function $f : \mathbb{R}^n \rightarrow \mathbb{R}^m$, the range of f is given by $\text{rge } f := \{y \mid \exists x \text{ with } y = f(x)\}$.

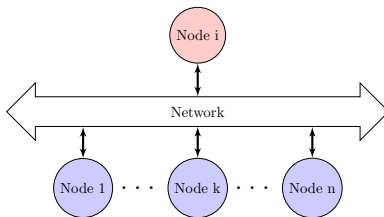


Figure 1: General architecture of the system under consideration.

2 Motivation for An Adaptive Clock Synchronization Algorithm

2.1 Preliminaries on the Sender-Receiver Algorithm

In a network of n nodes, consider nodes i and k in a sender-receiver hierarchy where Node i is a designated reference or parent agent of a synchronizing child agent Node k , see Figure 1. Each node has an attached internal clock $\tau_i, \tau_k \in \mathbb{R}$ whose dynamics are given by

$$\begin{aligned}\dot{\tau}_i &= a_i \\ \dot{\tau}_k &= a_k\end{aligned}\tag{1}$$

where $a_i, a_k \in \mathbb{R}$ denote the respective clock rates.¹ At times t_j for $j \in \mathbb{N}$ (with $t_0 = 0$), nodes i and k exchange timing measurements with embedded timestamps

$$\begin{aligned}T_j^i &:= \tau_i(t_j) \\ T_j^k &:= \tau_k(t_j)\end{aligned}\tag{2}$$

which, integrating (1), are equal to

$$\tau_i(t_j) = a_i t_j + \tau_i(0)$$

$$\tau_k(t_j) = a_k t_j + \tau_k(0)$$

respectively. Furthermore, $\tau_i(0)$ and $\tau_k(0)$ represent the clock offset from the initial reference time $t = 0$. The goal is to then synchronize the internal clock of Node k to that of Node i using the exchanged timing measurements given in (2).

Before introducing the mechanics of the sender-receiver algorithm, we refer the reader to a visual model of the algorithm in Figure 2 as a reference.

¹In this paper, we use the term clock rate to explicitly denote the slope of the given linear affine model of a clock. Other terms for this notion include clock drift or clock skew.

By assuming the sequence of time instants $\{t_j\}_{j=1}^{\infty}$ is strictly increasing and unbounded, the sender-receiver synchronization algorithm as described in the literature (see [7], [24], and [2]) is given as follows:

- (P1) At time t_j , Node i broadcasts a synchronization message with its local time

$$T_j^i = a_i t_j + \tau_i(0)$$

to Node k .

- (P2) At time t_{j+1} , Node k receives the synchronization message and records its local time of arrival, T_{j+1}^k , given in local time at

$$T_{j+1}^k = a_k t_{j+1} + \tau_k(0)$$

- (P3) At time t_{j+2} , Node k sends a response message with timestamp

$$T_{j+2}^k = a_k t_{j+2} + \tau_k(0)$$

- (P4) At time t_{j+3} , Node i receives the response message from Node k and records its time of arrival

$$T_{j+3}^i = a_i t_{j+3} + \tau_i(0)$$

- (P5) At time t_{j+4} , Node i sends a response receipt message with timestamp

$$T_{j+4}^i = a_i t_{j+4} + \tau_i(0)$$

- (P6) At time t_{j+5} , Node k receives the response message from Node i and records its time of arrival

$$T_{j+5}^k = a_k t_{j+5} + \tau_k(0)$$

and then updates its clock to synchronize with the clock of Node i using the collected timestamps T_j^i , T_{j+1}^k , T_{j+2}^k , T_{j+3}^i , and T_{j+4}^i .

Moreover, as done in the literature (see [24] and [9]), it is assumed that the time elapsed between each time instant is governed by

$$t_{j+1} - t_j = \begin{cases} d & \forall j \in \{2i + 1 : i \in \mathbb{N}\}, j > 0 \\ c & \forall j \in \{2i : i \in \mathbb{N}\}, j > 0 \end{cases} \quad (3)$$

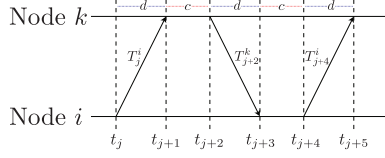


Figure 2: Diagram illustrating the message exchange between Nodes i and k for the synchronization algorithm.

where $0 < c \leq d$. The constant c defines the delay associated with the residence or response time associated with message turnaround while d defines the propagation delay associated with message transmission. Figure 2 gives a visual representation of the exchange of timestamps between Nodes i and k against reference time t . Note that the propagation delay from Node i to Node k and vice versa is assumed to be symmetric. Moreover, it is also assumed that the delay due to residence time is the same across all nodes.²

With the available timestamps, at times t_{j+5} , we can calculate the relative offset $\tilde{o} := \tau_i(0) - \tau_k(0)$ as follows, by first rearranging the terms in the timestamps given in (P1)-(P6) one has

$$\begin{aligned}
 \tau_i(0) &= T_j^i - a_i t_j \\
 \tau_k(0) &= T_{j+1}^k - a_k t_{j+1} \\
 \tau_k(0) &= T_{j+2}^k - a_k t_{j+2} \\
 \tau_i(0) &= T_{j+3}^i - a_i t_{j+3} \\
 \tau_i(0) &= T_{j+4}^i - a_i t_{j+4} \\
 \tau_k(0) &= T_{j+5}^k - a_k t_{j+5}
 \end{aligned}$$

then we have the following expressions for the offset

$$\begin{aligned}
 \tilde{o} = \tau_i(0) - \tau_k(0) &= T_j^i - a_i t_j - T_{j+1}^k + a_k t_{j+1} \\
 \tilde{o} = \tau_i(0) - \tau_k(0) &= T_{j+3}^i - a_i t_{j+3} - T_{j+2}^k + a_k t_{j+2} \\
 \tilde{o} = \tau_i(0) - \tau_k(0) &= T_{j+4}^i - a_i t_{j+4} - T_{j+5}^k + a_k t_{j+5}
 \end{aligned}$$

²Most pairwise synchronization protocols such as the Network Time Protocol (NTP), Precision Time Protocol (PTP, IEEE 1588), and the Timing-sync Protocol for Sensor Networks (TPSN) assume that the propagation delay in the message transmission from parent to child and child to parent is symmetric. If the propagation delay between the two nodes is asymmetric it introduces an error to the calculated offset correction that cannot be accounted for, see [16].

rearranging terms one has

$$\begin{aligned}
T_j^i - T_{j+1}^k &= a_i t_j - a_k t_{j+1} + \tilde{o} \\
T_{j+3}^i - T_{j+2}^k &= a_i t_{j+3} - a_k t_{j+2} + \tilde{o} \\
T_{j+4}^i - T_{j+5}^k &= a_i t_{j+4} - a_k t_{j+5} + \tilde{o}
\end{aligned} \tag{4}$$

Now, if the clock drifts are synchronized, i.e., $a_k = a_i$, we have

$$\begin{aligned}
T_j^i - T_{j+1}^k &= a_i(t_j - t_{j+1}) + \tilde{o} \\
T_{j+3}^i - T_{j+2}^k &= a_i(t_{j+3} - t_{j+2}) + \tilde{o} \\
T_{j+4}^i - T_{j+5}^k &= a_i(t_{j+4} - t_{j+5}) + \tilde{o}
\end{aligned} \tag{5}$$

then by noting the bounds on the time elapsed between time instants t_j , as given in (3), one has

$$t_{j+1} - t_j = t_{j+3} - t_{j+2} = t_{j+5} - t_{j+4} = d \quad \forall j \in \{2i + 1 : i \in \mathbb{N}\}, j > 0 \tag{6}$$

then by making the appropriate substitutions in (5) we have

$$\begin{aligned}
T_j^i - T_{j+1}^k &= -a_i d + \tilde{o} \\
T_{j+3}^i - T_{j+2}^k &= a_i d + \tilde{o} \\
T_{j+4}^i - T_{j+5}^k &= -a_i d + \tilde{o}
\end{aligned} \tag{7}$$

Since the clock rates $a_i = a_k$ and the quantity of the propagation delay d are currently unknowns to the system, we are left with a linear system of equations to solve for the offset, i.e.,

$$\tilde{o} = \frac{1}{2} \left((T_j^i - T_{j+1}^k) + (T_{j+3}^i - T_{j+2}^k) \right) \tag{8}$$

To demonstrate how this solves the synchronization problem, consider the error between the clocks of nodes i and k at t_{j+5} ,

$$e_{ik}(t_{j+5}) = \tau_i(t_{j+5}) - \tau_k(t_{j+5})$$

at time t_{j+5} node k applies the offset correction $K_{\tilde{o}} = \tilde{o}$ as follows

$$\begin{aligned}
e_{ik}(t_{j+5}) &= \tau_i(t_{j+5}) - (\tau_k(t_{j+5}) - K_{\tilde{o}}) \\
&= (a_i t_{j+5} + \tau_i(0)) - (a_k t_{j+5} + \tau_k(0) - (\tau_i(0) - \tau_k(0))) \\
&= a_i t_{j+5} - a_k t_{j+5} \\
&= 0
\end{aligned}$$

Thus, the clocks at nodes i and k synchronize for the case where the clock rates a_i and a_k are already assumed to be synchronized.

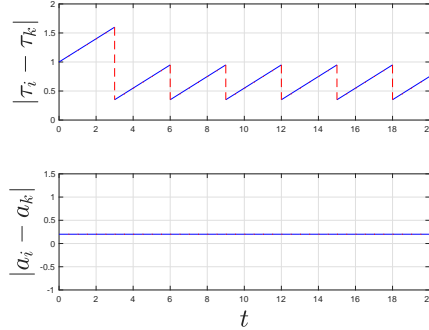


Figure 3: The evolution of the error in the clocks and error in the clock rates of Nodes i and k when the algorithm only applies the offset correction $K_{\tilde{\delta}}$.

2.2 The Key Issue: Clock synchronization in the presence of mismatched clock rates.

With the mechanics of the sender-receiver algorithm defined, we will now outline the motivation of this paper by demonstrating the issues that arise with the algorithm and how our proposed solution addresses them.

Now, consider the following system data $a_i = 1$, $a_k = 0.8$ with $c = d = 0.5$ and the given sender-receiver algorithm with only the offset correction $K_{\tilde{\delta}}$ being applied. Simulating the algorithm, Figure 3 shows the plots of the behavior in the error of clocks and the clock rates. As depicted in the figure, the algorithm continually applies the offset correction but due to the mismatch in the clock rates, the error in the clocks fails to converge to zero. This is further evidence analytically when noting that if the clock rates are not synchronized in equation (4), the formula for the offset calculation in (8) will yield an error on the true offset $\tilde{\delta}$.

To mitigate the effects of the error, protocols such as NTP and IEEE 1588 utilize a variety of bespoke methods to minimize the error in clock rates including but not limited to, control of variable frequency hardware oscillators, pulse addition and deletion of the counted pulses at the hardware oscillator, and an error register to track the deviation of the error, see [13] and [2]. These methods, while suitable for industrial-grade equipment, are often expensive solutions for low-cost applications such as sensor networks. In fact, protocols such as TPSN, designed specifically for low-cost sensor networks, do not provide provisions to correct for the clock rate error, see [15].

2.3 Problem Formulation and Proposed Algorithm

The problem to solve consists of synchronizing the internal clock of Node k to that of Node i . More precisely, the goal is to design a hybrid algorithm that is based on exchanging timestamps and guarantees that the clock variable τ_k and the clock rate a_k of Node k are driven to synchronization with τ_i and a_i of the reference Node i , respectively. Moreover, our goal is to provide tractable design conditions that ensure attractivity of a set of interest. This problem is formally stated as follows:

Problem 2.1. *Given two nodes in a sender-receiver hierarchy with clocks having dynamics as in (1) with timestamps T_j^i, T_j^k and parameters c and d , design a hybrid algorithm such that each trajectory $t \mapsto (\tau_i(t), \tau_k(t))$ satisfies the clock synchronization property*

$$\lim_{t \rightarrow \infty} |\tau_i(t) - \tau_k(t)| = 0$$

and the rate synchronization property

$$\lim_{t \rightarrow \infty} |\dot{\tau}_i(t) - \dot{\tau}_k(t)| = 0$$

Given the inability of the sender-receiver algorithm to synchronize the clocks, we propose a modification to the algorithm that incorporates an adaptive strategy to synchronize the clock rates. Consider the control law for the synchronization of the clock rate for Node k

$$K_a = \mu(T_{j+4}^i - T_j^i - T_{j+5}^k - T_{j+1}^k) \quad (9)$$

with $\mu > 0$ being a controllable parameter. Making the necessary substitutions one has

$$\begin{aligned} K_a &= \mu \left((a_i t_{j+4} + \tau_i(0)) - (a_i t_j + \tau_i(0)) \right. \\ &\quad \left. - (a_k t_{j+5} + \tau_k(0)) - (a_k t_{j+1} + \tau_k(0)) \right) \\ &= \mu (a_i (2c + 2d) - a_k (2c + 2d)) \\ &= \mu (2c + 2d) (a_i - a_k) \end{aligned} \quad (10)$$

The correction K_a can then be applied to the clock dynamics of Node k at times t_{j+5} as follows:

$$a_k^+ = a_k + K_a = a_k + \mu (2c + 2d) (a_i - a_k) \quad (11)$$

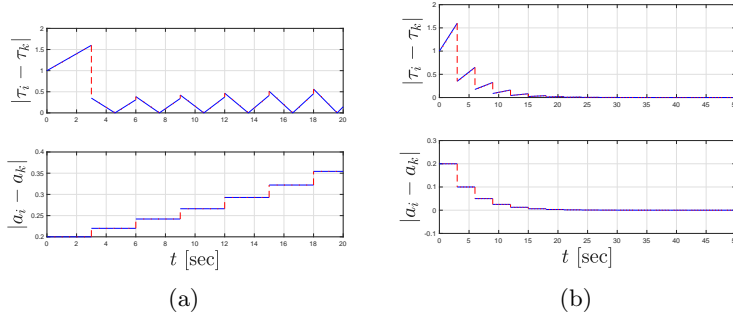


Figure 4: The evolution of the error in the clocks and clock rates of Nodes i and k when the algorithm applies both offset correction $K_{\bar{\sigma}}$ and clock rate correction K_a . Plot (a) demonstrates the case when μ is chosen arbitrarily while plot (b) depicts the scenario where μ is optimally chosen.

Observe that this strategy operates under the existing assumptions of the sender-receiver algorithm (symmetric propagation delays and residence times) and does not rely on any additional information that is not already available via the exchanged timing messages. Moreover, since it exploits the integrator dynamics of the system, the computation costs to calculate K_a are minimal. In this next example, we demonstrate the proposed strategy under the same scenario of mismatched skews between Nodes i and k .

To illustrate, the capabilities of the algorithm outlined above, consider the same system data as in Section 2, namely, $a_i = 1$, $a_k = 0.8$ with $c = d = 0.5$ and the given sender-receiver algorithm now with both the offset correction $K_{\bar{\sigma}}$ and clock rate correction K_a being applied. In Figure 4, two sets of error plots are presented for two different simulations. Figure 4(a) gives plots of the errors for the case where the μ is chosen using information on c and d following our forthcoming design conditions while Figure 4(b) provide the error plots for the case where μ is chosen arbitrarily. In the case of the ideal μ , the error in the clocks and clock rate converge to zero whereas in the case of the arbitrarily chosen μ , the error fails to converge. This suggests that a sufficient condition to appropriately design μ is necessary to ensure convergence of the error.

3 Preliminaries on Hybrid Systems

A hybrid system \mathcal{H} in \mathbb{R}^n is composed by the following *data*: a set $C \subset \mathbb{R}^n$, called the flow set; a set-valued mapping $F : \mathbb{R}^n \rightrightarrows \mathbb{R}^n$ with $C \subset \text{dom } F$,

called the flow map; a set $D \subset \mathbb{R}^n$, called the jump set; a set-valued mapping $G : \mathbb{R}^n \rightrightarrows \mathbb{R}^n$ with $D \subset \text{dom } G$, called the jump map. Then, a hybrid system $\mathcal{H} := (C, F, D, G)$ is written in the compact form

$$\mathcal{H} \begin{cases} \dot{x} \in F(x) & x \in C \\ x^+ \in G(x) & x \in D \end{cases} \quad (12)$$

where x is the system state. Solutions to hybrid systems are parameterized by (t, j) , where $t \in \mathbb{R}_{\geq 0}$ defines ordinary time and $j \in \mathbb{N}$ is a counter that defines the number of jumps. The evolution of ϕ is described by a *hybrid arc* on a *hybrid time domain* [22]. A hybrid time domain is given by $\text{dom } \phi \subset \mathbb{R}_{\geq 0} \times \mathbb{N}$ if, for each $(T, J) \in \text{dom } \phi$, $\text{dom } \phi \cap ([0, T] \times \{0, 1, \dots, J\})$ is of the form $\bigcup_{j=0}^J ([t_j, t_{j+1}] \times \{j\})$, with $0 = t_0 \leq t_1 \leq t_2 \leq t_{J+1}$. A solution ϕ is said to be *maximal* if it cannot be extended by flow or a jump, and *complete* if its domain is unbounded. For a hybrid system that is *well-posed*, the closed set $\mathcal{A} \subset \mathbb{R}^n$ is said to be: *attractive* for \mathcal{H} if there exists $\mu > 0$ such that every solution ϕ to \mathcal{H} with $|\phi(0, 0)|_{\mathcal{A}} \leq \mu$ is complete and satisfies $\lim_{t+j \rightarrow \infty} |\phi(t, j)|_{\mathcal{A}} = 0$.

4 A Hybrid Algorithm for Sender-Receiver Clock Synchronization

In this section we present our hybrid model that captures the network dynamics for the message exchange and our proposed algorithm that ensures synchronization of the clocks. Using the sender-receiver mechanism for exchanging the timing messages, our algorithm combines the offset correction law in (8) with the proposed online, adaptive clock rate correction law given in (9).

4.1 Modeling

Given the mix of continuous and discrete dynamics of the system, i.e., the continuous evolution of the clocks and the discrete events of the computation and network transmission, a hybrid modeling approach is a natural fit to perform the needed analysis and design goals to solve Problem 2.1. Thus, with our problem defined formally, we present a hybrid model that captures the proposed algorithm given in Section 2.3. To model the hardware and communication dynamics of the system, namely, the residence and transit times elapsed between the timing messages, we consider a global timer $\tau \in$

$[0, d]$ with dynamics

$$\begin{aligned} \dot{\tau} &= -1 & \tau &\in [0, d] \\ \tau^+ &\in \{c, d\} & \tau &= 0 \end{aligned} \quad (13)$$

In this model, the timer τ is reset to either c or d when $\tau = 0$ in order to preserve the bounds given in (3). We remind the reader that the constant c denotes the residence delay and d denotes the transmission or propagation delay. To determine the appropriate choice for the new value of τ , namely, τ^+ , we define a discrete variable $q \in \{0, 1\} =: \mathcal{Q}$ to indicate the residence or transmission state of the system, namely, whether the system is servicing a message at one of the two nodes or whether the system is waiting for the arrival of a message at either of the two nodes, respectively. The state vectors

$$m^i = [m_1^i, m_2^i, m_3^i, m_4^i, m_5^i, m_6^i]^\top \in \mathbb{R}^6$$

and

$$m^k = [m_1^k, m_2^k, m_3^k, m_4^k, m_5^k, m_6^k]^\top \in \mathbb{R}^6$$

represent memory buffers to store the received and transmitted timestamps respectively, for Node i and Node k . In addition, a second discrete variable $p \in \{0, 1, 2, 3, 4, 5\} =: \mathcal{P}$ is used to track at which stage of the message exchange, defined in (P1)-(P6), the algorithm is at. Then, by incorporating the clocks τ_i, τ_k and the clock rates a_i, a_k as state variables to the model as in Section 2.1, the state x of the hybrid system model, denoted \mathcal{X} , is given by

$$x := (\tau_i, \tau_k, a_i, a_k, \tau, m^i, m^k, p, q) \in \mathcal{X}$$

where

$$\mathcal{X} := \mathbb{R} \times \mathbb{R} \times \mathbb{R} \times \mathbb{R} \times [0, d] \times \mathbb{R}^6 \times \mathbb{R}^6 \times \mathcal{P} \times \mathcal{Q}$$

With the dynamics of the clocks as given in (1) and those of the timer τ in (13), the flow map is defined as

$$F(x) := (a_i, a_k, 0, 0, -1, 0, 0, 0, 0) \quad \forall x \in C \quad (14)$$

the flow set C is defined as

$$C := C_1 \cup C_2 \quad (15)$$

where

$$C_1 := \{x \in \mathcal{X} : q = 0, \tau \in [0, c]\}$$

and

$$C_2 := \{x \in \mathcal{X} : q = 1, \tau \in [0, d]\}$$

To model the communication and arrival events of the message exchange and the proposed mechanisms correcting the clock rate and offset, we define the jump map $G : \mathbb{R}^n \rightarrow \mathbb{R}^n$ as

$$G(x) := G_i(x) \text{ if } x \in D_i \quad (16)$$

where each mapping G_i used to define G corresponds to the message exchange events (P1)-(P6) as follows

- G_1 : Node i broadcasts a synchronization message to Node k timestamped with τ_i as in (P1). This event is triggered by the jump set D_1 , namely, when the timer $\tau = 0$ and the discrete variable p describing the protocol state is zero. At this event, the timer τ is reset to d , to initiate the message transmission delay. Similarly, the state q is reset to 1 to indicate the message transmission state of the system with p augmented by one to trigger the next protocol state. Finally, m_1^i is set to τ_i to record the time of message broadcast, relative to the clock of Node i . The subsequent memory states m_2^i, \dots, m_6^i are reset to m_1^i, \dots, m_5^i , respectively.
- G_2 : Node k receives the synchronization message and timestamps its arrival with τ_k as in (P2). This event is triggered by the jump set D_2 , namely, when the timer $\tau = 0$ and the discrete variable p describing the protocol state is one. At this event, the timer τ is reset to c , to initiate the residence delay. Similarly, the state q is reset to 0 to indicate the residence state of the system. Finally, m_1^k is set to τ_k to record the time of message broadcast, relative to the clock of Node i . The subsequent memory states m_2^k, \dots, m_6^k are reset to m_1^i, \dots, m_5^i , respectively.
- G_3 : Node k broadcasts a response message timestamped with τ_k as in (P3). This event is triggered by the jump set D_3 , namely, when the timer $\tau = 0$ and the discrete variable p describing the protocol state is two. At this event, the timer τ is reset to d , to initiate the message transmission delay. Similarly, the state q is reset to 1 to indicate the message transmission state of the system. Finally, m_1^i is set to τ_i to record the time of message broadcast, relative to the clock of Node i . The subsequent memory states m_2^i, \dots, m_6^i are reset to m_1^i, \dots, m_5^i , respectively.
- G_4 : Node i receives the response message and timestamps its arrival with τ_k as in (P4). This event is triggered by the jump set D_4 , namely,

when the timer $\tau = 0$ and the discrete variable p describing the protocol state is three. At this event, the timer τ is reset to c , to initiate the residence delay. Similarly, the state q is reset to 0 to indicate the residence state of the system. Finally, m_1^k is set to τ_k to record the time of message broadcast, relative to the clock of Node i . The subsequent memory states m_2^k, \dots, m_6^k are reset to m_1^i, \dots, m_5^i , respectively.

- G_5 : Node i broadcasts a response receipt message timestamped with τ_i as in (P5). This event is triggered by the jump set D_5 , namely, when the timer $\tau = 0$ and the discrete variable p describing the protocol state is four. At this event, the timer τ is reset to d , to initiate the message transmission delay. Similarly, the state q is reset to 1 to indicate the message transmission state of the system. Finally, m_1^i is set to τ_i to record the time of message broadcast, relative to the clock of Node i . The subsequent memory states m_2^i, \dots, m_6^i are reset to m_1^i, \dots, m_5^i , respectively.
- G_6 : Node k uses the timestamped messages to update its clock rate and offset via $K_{\bar{\delta}}(x)$ in (8) and $K_a(x)$ in (18), respectively as in (P6). This event is triggered by the jump set D_6 , namely, when the timer $\tau = 0$ and the discrete variable p describing the protocol state is five. At this event, the timer τ is reset to c , to initiate the residence delay. Similarly, the state q is reset to 0 to indicate the residence state of the system. Finally, m_1^k is set to τ_k to record the time of message broadcast, relative to the clock of Node i . The subsequent memory states m_2^k, \dots, m_6^k are reset to m_1^i, \dots, m_5^i , respectively.

More precisely, the maps $G_1, G_2, G_3, G_4, G_5, G_6$, updating $x = (\tau_i, \tau_k, a_i, a_k, \tau, m^i, m^k, p, q)$, are defined by³

$$\begin{aligned}
G_1(x) &:= \begin{bmatrix} (\tau_i, \tau_k) \\ (a_i, a_k) \\ d \\ (\tau_i, m_1^i, \dots, m_5^i), m^k \\ p+1 \\ 1 \end{bmatrix}, & G_2(x) &:= \begin{bmatrix} (\tau_i, \tau_k) \\ (a_i, a_k) \\ c \\ (m^i, \tau_k, m_1^i, \dots, m_5^i) \\ p+1 \\ 0 \end{bmatrix} \\
G_3(x) &:= \begin{bmatrix} (\tau_i, \tau_k) \\ (a_i, a_k) \\ d \\ (m^i, \tau_k, m_1^k, \dots, m_5^k) \\ p+1 \\ 1 \end{bmatrix}, & G_4(x) &:= \begin{bmatrix} (\tau_i, \tau_k) \\ (a_i, a_k) \\ c \\ (\tau_i, m_1^k, \dots, m_5^k, m^k) \\ p+1 \\ 0 \end{bmatrix} \\
G_5(x) &:= \begin{bmatrix} (\tau_i, \tau_k) \\ (a_i, a_k) \\ d \\ (\tau_i, m_1^i, \dots, m_5^i, m^k) \\ p+1 \\ 1 \end{bmatrix}, & G_6(x) &:= \begin{bmatrix} (\tau_i, \tau_k - K_{\bar{o}}(m^i)) \\ (a_i, a_k + K_a(m^i, \tau_k)) \\ c \\ (m^i, \tau_k, m_1^i, \dots, m_5^i) \\ 0 \\ 0 \end{bmatrix}
\end{aligned} \tag{17}$$

with

$$K_{\bar{o}}(m^i) = \frac{1}{2}(m_4^i - m_5^i - m_2^i + m_3^i) \tag{18}$$

and

$$K_a(m^i, \tau_k) = \mu((m_1^i - m_5^i) - (\tau_k - m_4^i)) \tag{19}$$

with $\mu > 0$. The offset correction implemented by the feedback law $K_{\bar{o}}$ in (18) is an adapted version of the offset correction algorithm given in (8) suitable for the hybrid system model where the memory states m^i and m^k contain the stored timestamps T_j^i and T_j^k , respectively. Note that the feedback laws $K_{\bar{o}}$ and K_a depend on the correct assignment of the timestamps to the memory states. In the forthcoming Lemmas 4.3 and 4.4, we show finite time attractivity of a set containing the correct assignment of the memory states for the appropriate feedback. To trigger the jumps corresponding to the particular protocol events (P1)-(P6), we define the jump set as

$$D := D_1 \cup D_2 \cup D_3 \cup D_4 \cup D_5 \cup D_6$$

³Note that $[x^\top, y^\top]^\top = (x, y)$.

where

$$\begin{aligned} D_1 &:= \{x \in \mathcal{X} : \tau = 0, p = 0\}, & D_2 &:= \{x \in \mathcal{X} : \tau = 0, p = 1\} \\ D_3 &:= \{x \in \mathcal{X} : \tau = 0, p = 2\}, & D_4 &:= \{x \in \mathcal{X} : \tau = 0, p = 3\} \\ D_5 &:= \{x \in \mathcal{X} : \tau = 0, p = 4\}, & D_6 &:= \{x \in \mathcal{X} : \tau = 0, p = 5\} \end{aligned}$$

With the data defined, we let $\mathcal{H} = (C, F, D, G)$ denote the hybrid system for the pairwise broadcast synchronization algorithm between Node i and Node k .

4.2 Error Model

To show that the proposed algorithm solves Problem 2.1, we recast the problem as a set stabilization problem. Namely, we show that solutions ϕ to \mathcal{H} , with data (C, F, D, G) given in (12), converge to a set of interest wherein the clock states τ_i, τ_k and clock rates a_i, a_k , respectively, coincide. To this end, we consider an augmented model of \mathcal{H} in error coordinates to capture such a property. Let $\varepsilon := (\varepsilon_\tau, \varepsilon_a) \in \mathbb{R}^2$, where $\varepsilon_\tau := \tau_i - \tau_k$ defines the clock error and $\varepsilon_a := a_i - a_k$ defines the clock rate error of Nodes i and k . Then, define

$$x_\varepsilon := (\varepsilon, x) \in \mathcal{X}_\varepsilon := \mathbb{R}^2 \times \mathcal{X}$$

which is the state⁴ that collects the clock errors, clock rate errors, and the state of the system \mathcal{H} . The continuous evolution of x_ε is governed by

$$\dot{x}_\varepsilon = F_\varepsilon(x_\varepsilon) := (A_f \varepsilon, F(x)) \quad x_\varepsilon \in C_\varepsilon \quad (20)$$

where $A_f = \begin{bmatrix} 0 & 1 \\ 0 & 0 \end{bmatrix}$ and f is defined in (14). The flow set C_ε is defined as

$$C_\varepsilon := C_{\varepsilon_1} \cup C_{\varepsilon_2} \quad (21)$$

where

$$C_{\varepsilon_1} := \{x_\varepsilon \in \mathcal{X}_\varepsilon : q = 0, \tau \in [0, c]\}$$

and

$$C_{\varepsilon_2} := \{x_\varepsilon \in \mathcal{X}_\varepsilon : q = 1, \tau \in [0, d]\}$$

The discrete changes of x_ε are determined by the discrete changes of ε and x , the latter of which is given in (16). Through the computation of $\varepsilon^+ =$

⁴The full state vector x to \mathcal{H} is retained to facilitate the implementation of the synchronization algorithm for \mathcal{H}_ε .

$(\varepsilon_\tau^+, \varepsilon_a^+)$ using the jump maps in (17), the resulting evolution is modeled by the jump map $G_\varepsilon : \mathcal{X}_\varepsilon \rightarrow \mathcal{X}_\varepsilon$ given by

$$G_\varepsilon(x_\varepsilon) := G_{\varepsilon_i}(x_\varepsilon) \quad \text{if } x_\varepsilon \in D_{\varepsilon_i} \quad (22)$$

where

$$\begin{aligned} G_{\varepsilon_1}(x_\varepsilon) &:= \begin{bmatrix} \varepsilon \\ G_1(x) \end{bmatrix}, \quad G_{\varepsilon_2}(x_\varepsilon) := \begin{bmatrix} \varepsilon \\ G_2(x) \end{bmatrix}, \quad G_{\varepsilon_3}(x_\varepsilon) := \begin{bmatrix} \varepsilon \\ G_3(x) \end{bmatrix} \\ G_{\varepsilon_4}(x_\varepsilon) &:= \begin{bmatrix} \varepsilon \\ G_4(x) \end{bmatrix}, \quad G_{\varepsilon_5}(x_\varepsilon) := \begin{bmatrix} \varepsilon \\ G_5(x) \end{bmatrix}, \quad G_{\varepsilon_6}(x_\varepsilon) := \begin{bmatrix} \varepsilon + \begin{bmatrix} K_{\bar{\delta}}(m^i) \\ -K_a(m^i, \tau_k) \end{bmatrix} \\ G_6(x) \end{bmatrix} \end{aligned}$$

Observe that the feedback laws $K_{\bar{\delta}}$ and K_a are employed when ε is updated by G_{ε_6} , similarly to when G_6 is employed \mathcal{H} . These discrete dynamics apply when x is in $D_\varepsilon := D_{\varepsilon_1} \cup D_{\varepsilon_2} \cup D_{\varepsilon_3} \cup D_{\varepsilon_4} \cup D_{\varepsilon_5} \cup D_{\varepsilon_6}$, where

$$\begin{aligned} D_{\varepsilon_1} &:= \{x_\varepsilon \in \mathcal{X}_\varepsilon : \tau = 0, p = 0\}, & D_{\varepsilon_2} &:= \{x_\varepsilon \in \mathcal{X}_\varepsilon : \tau = 0, p = 1\} \\ D_{\varepsilon_3} &:= \{x_\varepsilon \in \mathcal{X}_\varepsilon : \tau = 0, p = 2\}, & D_{\varepsilon_4} &:= \{x_\varepsilon \in \mathcal{X}_\varepsilon : \tau = 0, p = 3\} \\ D_{\varepsilon_5} &:= \{x_\varepsilon \in \mathcal{X}_\varepsilon : \tau = 0, p = 4\}, & D_{\varepsilon_6} &:= \{x_\varepsilon \in \mathcal{X}_\varepsilon : \tau = 0, p = 5\} \end{aligned}$$

This hybrid system is denoted

$$\mathcal{H}_\varepsilon = (C_\varepsilon, F_\varepsilon, D_\varepsilon, G_\varepsilon) \quad (23)$$

The set to render attractive so as to solve Problem 2.1 is given by

$$\mathcal{A}_\varepsilon := \{x_\varepsilon \in \mathcal{X}_\varepsilon : \varepsilon = 0\} \quad (24)$$

where $\varepsilon = 0$ implies synchronization of both the clock offset and the clock rate, since, when $\varepsilon_\tau = 0$ and $\varepsilon_a = 0$, then τ_k is synchronized to τ_i .

4.3 Basic Properties of \mathcal{H}_ε

Having the hybrid system \mathcal{H}_ε defined, the next two results establish existence of solutions to \mathcal{H}_ε and that every maximal solution to \mathcal{H}_ε is complete. In particular, we show that, through the satisfaction of some basic conditions on the hybrid system data, which is shown first, the system \mathcal{H}_ε is well-posed and that each maximal solution to the system is defined for arbitrarily large $t + j$.

Lemma 4.1. *The hybrid system $\mathcal{H}_\varepsilon = (C_\varepsilon, F_\varepsilon, D_\varepsilon, G_\varepsilon)$ satisfies the following conditions, defined in [22, Assumption 6.5] as the hybrid basic conditions; namely,*

(A1) C_ε and D_ε are closed subsets of \mathbb{R}^m ;

(A2) $F_\varepsilon : \mathbb{R}^m \rightarrow \mathbb{R}^m$ is continuous;

(A3) $G_\varepsilon : \mathbb{R}^m \rightrightarrows \mathbb{R}^m$ is outer semicontinuous and locally bounded relative to D_ε , and $D_\varepsilon \subset \text{dom } G_\varepsilon$.

Proof. By inspection of the hybrid system data $(C_\varepsilon, F_\varepsilon, D_\varepsilon, G_\varepsilon)$ defining \mathcal{H}_ε given in (23), the following is observed:

- The set C_ε is a closed subset of \mathbb{R}^m since C_ε is the union of the sets C_{ε_1} and C_{ε_2} , both of which are the Cartesian product of closed sets. Similar arguments show that D_ε is closed since it can be written as the finite union of closed sets, that is,

$$D_\varepsilon = \bigcup_{p \in \mathcal{P}} (\mathbb{R}^2 \times \mathbb{R} \times \mathbb{R} \times \mathbb{R} \times \mathbb{R} \times \{0\} \times \mathbb{R}^6 \times \mathbb{R}^6 \times \{p\} \times \mathcal{Q})$$

Thus, (A1) holds.

- The function $F_\varepsilon : \mathcal{X}_\varepsilon \rightarrow \mathcal{X}_\varepsilon$ is linear affine in the state and thus continuous on C_ε . Thus, (A2) holds.
- To show that the set-valued map G_ε defined in (22) satisfies (A3), observe that by inspection, for each $i \in \{1, 2, 3, 4, 5, 6\}$ G_{ε_i} is a continuous map. Moreover, for each $i \in \{1, 2, 3, 4, 5, 6\}$ D_{ε_i} is closed and

$$D_{\varepsilon_i} \cap D_{\varepsilon_k} = \emptyset \quad \forall i, k \in \{1, 2, 3, 4, 5, 6\}, i \neq k$$

which implies that there is a (uniform) finite separation between these sets. This is due to the fact that these sets are defined for different values of the logic variables. Hence, (A3) holds as G_ε is a piecewise function with each piece being continuous.

□

Lemma 4.2. *For every $\xi \in C_\varepsilon \cup D_\varepsilon (= \mathcal{X}_\varepsilon)$, there exists at least one non-trivial solution ϕ to \mathcal{H}_ε such that $\phi(0, 0) = \xi$. Moreover, every maximal solution to \mathcal{H}_ε is complete.*

Proof. Consider an arbitrary $\xi \in C_\varepsilon \cup D_\varepsilon$. The tangent cone $T_{C_\varepsilon}(\xi)$, as defined in [22, Definition 5.12], given by

$$T_{C_\varepsilon}(\xi) = \begin{cases} \mathbb{R}^2 \times \mathbb{R} \times \mathbb{R} \times \mathbb{R} \times \mathbb{R} \times \mathbb{R}_{\geq 0} \times \mathbb{R}^6 \times \mathbb{R}^6 \times \mathcal{P} \times \mathcal{Q} & \text{if } \xi \in \mathcal{X}_\varepsilon^1 \\ \mathbb{R}^2 \times \mathbb{R} \times \mathbb{R} \times \mathbb{R} \times \mathbb{R} \times \mathbb{R} \times \mathbb{R}^6 \times \mathbb{R}^6 \times \mathcal{P} \times \mathcal{Q} & \text{if } \xi \in \mathcal{X}_\varepsilon^2 \\ \mathbb{R}^2 \times \mathbb{R} \times \mathbb{R} \times \mathbb{R} \times \mathbb{R} \times \mathbb{R}_{\leq 0} \times \mathbb{R}^6 \times \mathbb{R}^6 \times \mathcal{P} \times \mathcal{Q} & \text{if } \xi \in \mathcal{X}_\varepsilon^3 \end{cases}$$

where $\mathcal{X}_\varepsilon^1 := \{x_\varepsilon \in \mathcal{X}_\varepsilon : \tau = 0\}$, $\mathcal{X}_\varepsilon^2 := \{x_\varepsilon \in \mathcal{X}_\varepsilon : \tau \in (0, d)\}$, and $\mathcal{X}_\varepsilon^3 := \{x_\varepsilon \in \mathcal{X}_\varepsilon : \tau = d\}$. By inspection, $F_\varepsilon(x_\varepsilon) \cap T_{C_\varepsilon}(x_\varepsilon) \neq \emptyset$ holds for every $x_\varepsilon \in C_\varepsilon \setminus D$. Then, by [22, Proposition 6.10], there exists a nontrivial solution ϕ to \mathcal{H}_ε with $\phi(0, 0) = \xi$. Moreover, by the same result, every $\phi \in \mathcal{S}_{\mathcal{H}_\varepsilon}$ satisfies one of the following conditions:

- a) ϕ is complete;
- b) $\text{dom } \phi$ is bounded and the interval I^J , where $J = \sup_j \text{dom } \phi$, has nonempty interior and $t \mapsto \phi(t, J)$ is a maximal solution to $\dot{x} \in F(x)$, in fact $\lim_{t \rightarrow T} |\phi(t, J)| = \infty$, where $T = \sup_t \text{dom } \phi$;
- c) $\phi(T, J) \notin C \cup D$, where $(T, J) = \sup \text{dom } \phi$.

Now, since $G_\varepsilon(D_\varepsilon) \subset C_\varepsilon \cup D_\varepsilon$ case (c) does not occur. Additionally, one can eliminate case (b) since, by inspection, F_ε is Lipschitz continuous on C_ε . \square

The effectiveness of the update laws K_δ and K_a , given in (18) and (19), in correcting the clock and clock rate of Node k , depend on the assigned values of m^i and m^k at the time K_δ and K_a , i.e., when jumps according to G_{ε_6} occur. Improper initialization of the memory states may result in updates of the offset and clock rate of Node k that increase the error in the clocks and clock rates relative to Node i . Therefore, to facilitate the analysis of \mathcal{H}_ε in rendering the set \mathcal{A}_ε asymptotically attractive, we restrict the values of m^i and m^k to a set smaller than \mathcal{X} where they remain in forward (hybrid) time. More precisely, we restrict the state x_ε to the set

$$\mathcal{M} := \mathcal{M}_1 \cup \mathcal{M}_2 \cup \mathcal{M}_3 \cup \mathcal{M}_4 \cup \mathcal{M}_5 \cup \mathcal{M}_6 \quad (25)$$

where

$$\begin{aligned}
\mathcal{M}_1 &:= \{x_\varepsilon \in \mathcal{X}_\varepsilon : p=0, q=0\} \\
\mathcal{M}_2 &:= \{x_\varepsilon \in \mathcal{X}_\varepsilon : p=1, q=1, m_1^i - \rho_i(x_\varepsilon, 0) = 0\} \\
\mathcal{M}_3 &:= \{x_\varepsilon \in \mathcal{X}_\varepsilon : p=2, q=0, m_1^k - \rho_k(x_\varepsilon, 0) = 0, \\
&\quad m_2^k - \rho_i(x_\varepsilon, d) = 0\} \\
\mathcal{M}_4 &:= \{x_\varepsilon \in \mathcal{X}_\varepsilon : p=3, q=1, m_1^k - \rho_k(x_\varepsilon, 0) = 0, \\
&\quad m_2^k - \rho_k(x_\varepsilon, c) = 0, m_3^k - \rho_i(x_\varepsilon, c+d) = 0\} \\
\mathcal{M}_5 &:= \{x_\varepsilon \in \mathcal{X}_\varepsilon : p=4, q=0, m_1^i - \rho_i(x_\varepsilon, 0) = 0, \\
&\quad m_2^i - \rho_k(x_\varepsilon, d) = 0, m_3^i - \rho_k(x_\varepsilon, c+d) = 0, \\
&\quad m_4^i - \rho_i(x_\varepsilon, 2d+c) = 0\} \\
\mathcal{M}_6 &:= \{x_\varepsilon \in \mathcal{X}_\varepsilon : p=5, q=1, m_1^i - \rho_i(x_\varepsilon, 0) = 0, \\
&\quad m_2^i - \rho_i(x_\varepsilon, c) = 0, m_3^i - \rho_k(x_\varepsilon, c+d) = 0, \\
&\quad m_4^i - \rho_k(x_\varepsilon, 2c+d) = 0, m_5^i - \rho_i(x_\varepsilon, 2c+2d) = 0\}
\end{aligned}$$

and

$$\begin{aligned}
\rho_i(x_\varepsilon, \beta) &:= \tau_i - a_i((1-q)c + qd - \tau) - a_i\beta \\
\rho_k(x_\varepsilon, \beta) &:= \tau_k - a_k((1-q)c + qd - \tau) - a_k\beta
\end{aligned} \tag{26}$$

for $\beta \geq 0$.

Lemma 4.3. *The set \mathcal{M} is forward invariant for the hybrid system \mathcal{H}_ε .*

Proof. Pick an initial condition $\phi(0, 0) \in \mathcal{M}$.

- If $\phi(0, 0) \in \mathcal{M} \cap (C_\varepsilon \setminus D_\varepsilon)$, then the solution initially flows according to $\dot{x}_\varepsilon = F_\varepsilon(x)$. Observe that the trajectories of m^i , m^k , p , and q remain constant since F_ε is defined so that $\dot{m}^i = \dot{m}^k = \dot{p} = \dot{q} = 0$. Moreover, note that the gradient of ρ_i and ρ_k with respect to $x_\varepsilon =$

$(\varepsilon, \tau_i, \tau_k, a_i, a_k, \tau, m^i, m^k, p, q)$ satisfy

$$\nabla_{x_\varepsilon} \rho_i(x_\varepsilon, \beta) = \begin{bmatrix} \mathbf{0}_{2 \times 1} \\ 1 \\ 0 \\ \tau - \beta - dq + c(q-1) \\ 0 \\ a_i \\ \mathbf{0}_{6 \times 1} \\ \mathbf{0}_{6 \times 1} \\ 0 \\ a_i(c-d) \end{bmatrix}, \quad \nabla_{x_\varepsilon} \rho_k(x_\varepsilon, \beta) = \begin{bmatrix} \mathbf{0}_{2 \times 1} \\ 0 \\ 1 \\ 0 \\ \tau - \beta - dq + c(q-1) \\ a_k \\ \mathbf{0}_{6 \times 1} \\ \mathbf{0}_{6 \times 1} \\ 0 \\ a_k(c-d) \end{bmatrix} \quad (27)$$

Then one has $\dot{\rho}_i(x_\varepsilon, \beta) = \langle \nabla \rho_i(x_\varepsilon, \beta), F_\varepsilon(x_\varepsilon) \rangle = 1a_i + a_i(-1) = 0$ and $\dot{\rho}_k(x_\varepsilon, \beta) = \langle \nabla \rho_k(x_\varepsilon, \beta), F_\varepsilon(x_\varepsilon) \rangle = 1a_k + a_k(-1) = 0$. Therefore, when ϕ initially flows from a point in \mathcal{M} , it remains in \mathcal{M} over the interval of flow. This property holds for every solution over any of its intervals of flows that starts at a point in \mathcal{M} .

- If $\phi(0, 0) \in \mathcal{M} \cap D_\varepsilon$, then the solution initially jumps according to $x_\varepsilon^+ = G_\varepsilon(x_\varepsilon)$. In particular,
 - if $\phi(0, 0) \in \mathcal{M}_1 \cap D_{\varepsilon_1}$, the solution jumps according to $x_\varepsilon^+ = G_{\varepsilon_1}(x_\varepsilon)$. The timer τ resets according to $\tau^+ = d$ while $q^+ = 1$ and $p^+ = 1$. Moreover, $(m_1^i)^+$ is assigned to the value of τ_i , evaluating $\rho_i(x_\varepsilon^+, 0)$, we have that for each $x_\varepsilon \in D_{\varepsilon_1}$

$$\begin{aligned} \rho_i(x_\varepsilon^+, 0) &= \tau_i - a_i((1 - q^+)c + q^+d - \tau^+) - a_i 0 \\ &= \tau_i - a_i((1 - 1)c + d - d) \\ &= \tau_i \end{aligned}$$

Thus, by recalling the definition of $\mathcal{M}_2 = \{x_\varepsilon \in \mathcal{X}_\varepsilon : p=1, q=1, m_1^i - \rho_i(x_\varepsilon, 0) = 0\}$, we have that $G_{\varepsilon_1}(\mathcal{M}_1 \cap D_\varepsilon) \subset \mathcal{M}_2$ holds for each $x_\varepsilon \in D_{\varepsilon_1}$.

- if $\phi(0, 0) \in \mathcal{M}_2 \cap D_\varepsilon$, the solution jumps according to $x_\varepsilon^+ = G_{\varepsilon_2}(x_\varepsilon)$. The timer τ resets according to $\tau^+ = c$ while $q^+ = 0$ and $p^+ = 2$. Then, by definition of G_{ε_2} , for each $x_\varepsilon \in D_{\varepsilon_2}$, one has

$$\begin{aligned} \rho_k(x_\varepsilon^+, 0) &= \tau_k - a_k((1 - q^+)c + q^+d - \tau^+) - a_k 0 \\ &= \tau_k - a_k((1 - 0)c - c) \\ &= \tau_k \end{aligned}$$

which is equal to $(m_1^k)^+$ and

$$\begin{aligned}\rho_i(x_\varepsilon^+, d) &= \tau_i - a_i((1 - q^+)c + q^+d - \tau^+) - a_id \\ &= \tau_i - a_i((1 - 0)c - c) - a_id \\ &= \tau_i - a_id\end{aligned}$$

which is equal to $(m_2^k)^+ = m_1^i$. Therefore, by recalling the definition $\mathcal{M}_3 = \{x_\varepsilon \in \mathcal{X}_\varepsilon : p=2, q=0, m_1^k - \rho_k(x_\varepsilon, 0) = 0, m_2^k - \rho_i(x_\varepsilon, d) = 0\}$, we have $G_{\varepsilon_2}(\mathcal{M}_2 \cap D_\varepsilon) \subset \mathcal{M}_3$ for each $x_\varepsilon \in D_{\varepsilon_2}$.

- if $\phi(0, 0) \in \mathcal{M}_3 \cap D_\varepsilon$, the solution jumps according to $x_\varepsilon^+ = G_{\varepsilon_3}(x_\varepsilon)$. The timer τ resets according to $\tau^+ = d$ while $q^+ = 1$ and $p^+ = 3$. Then, by definition of G_{ε_3} , for each $x_\varepsilon \in D_{\varepsilon_3}$, one has

$$\begin{aligned}\rho_k(x_\varepsilon^+, 0) &= \tau_k - a_k((1 - q^+)c + qd - \tau^+) - a_k0 \\ &= \tau_k - a_k((1 - 1)c + d - d) \\ &= \tau_k\end{aligned}$$

which is equal to $(m_1^k)^+$,

$$\begin{aligned}\rho_k(x_\varepsilon^+, c) &= \tau_k - a_k((1 - q^+)c + qd - \tau^+) - a_kc \\ &= \tau_k - a_k((1 - 1)c + d - d) - a_kc \\ &= \tau_k - a_kc\end{aligned}$$

which is equal to $(m_2^k)^+ = m_1^k$, and

$$\begin{aligned}\rho_i(x_\varepsilon^+, c + d) &= \tau_i - a_i((1 - q^+)c + qd - \tau^+) - a_i(c + d) \\ &= \tau_i - a_i((1 - 1)c + d - d) - a_i(c + d) \\ &= \tau_i - a_i(c + d)\end{aligned}$$

which is equal to $(m_3^k)^+ = m_2^k$. Therefore, by recalling the definition $\mathcal{M}_4 = \{x_\varepsilon \in \mathcal{X}_\varepsilon : p=3, q=1, m_1^k - \rho_k(x_\varepsilon, 0) = 0, m_2^k - \rho_k(x_\varepsilon, c) = 0, m_3^k - \rho_i(x_\varepsilon, c + d) = 0\}$, we have $G_{\varepsilon_3}(\mathcal{M}_3 \cap D_\varepsilon) \subset \mathcal{M}_4$ for each $x_\varepsilon \in D_{\varepsilon_3}$.

- if $\phi(0, 0) \in \mathcal{M}_4 \cap D_\varepsilon$, the solution jumps according to $x_\varepsilon^+ = G_{\varepsilon_4}(x_\varepsilon)$. The timer τ resets according to $\tau^+ = c$ while $q^+ = 0$ and $p^+ = 4$. Then, by definition of G_{ε_4} , for each $x_\varepsilon \in D_{\varepsilon_4}$, one has

$$\begin{aligned}\rho_i(x_\varepsilon^+, 0) &= \tau_i - a_i((1 - q^+)c + qd - \tau^+) - a_i\beta \\ &= \tau_i - a_i((1 - 0)c - c) \\ &= \tau_i\end{aligned}$$

which is equal to $(m_1^k)^+$,

$$\begin{aligned}\rho_k(x_\varepsilon^+, d) &= \tau_k - a_k((1 - q^+)c + qd - \tau^+) - a_k d \\ &= \tau_k - a_k((1 - 0)c - c) - a_k d \\ &= \tau_k - a_k d\end{aligned}$$

which is equal to $(m_2^i)^+ = m_1^k$,

$$\begin{aligned}\rho_k(x_\varepsilon^+, c + d) &= \tau_k - a_k((1 - q^+)c + qd - \tau^+) - a_k(c + d) \\ &= \tau_k - a_k((1 - 0)c - c) - a_k(c + d) \\ &= \tau_k - a_k(c + d)\end{aligned}$$

which is equal to $(m_3^i)^+ = m_2^i$,

$$\begin{aligned}(m_4^i)^+ &= m_3^k = \rho_i(x_\varepsilon^+, c + 2d) \\ &= \tau_i - a_i((1 - q^+)c + qd - \tau^+) - a_i(c + 2d) \\ &= \tau_i - a_i((1 - 0)c - c) - a_i(c + 2d) \\ &= \tau_i - a_i(c + 2d)\end{aligned}$$

which is equal to $(m_4^i)^+ = m_3^k$. Therefore, by recalling the definition $\mathcal{M}_5 = \{x_\varepsilon \in \mathcal{X}_\varepsilon : p=4, q=0, m_1^i - \rho_i(x_\varepsilon, 0) = 0, m_2^i - \rho_k(x_\varepsilon, d) = 0, m_3^i - \rho_k(x_\varepsilon, c+d) = 0, m_4^i - \rho_i(x_\varepsilon, c+2d)=0\}$, we have $G_{\varepsilon_4}(\mathcal{M}_4 \cap D_\varepsilon) \subset \mathcal{M}_5$ for each $x_\varepsilon \in D_{\varepsilon_4}$.

– if $\phi(0, 0) \in \mathcal{M}_5 \cap D_\varepsilon$, the solution jumps according to $x_\varepsilon^+ = G_{\varepsilon_5}(x_\varepsilon)$. The timer τ resets according to $\tau^+ = d$ while $q^+ = 1$ and $p^+ = 5$. Then, by definition of G_{ε_5} , for each $x_\varepsilon \in D_{\varepsilon_5}$, one has

$$\begin{aligned}\rho_i(x_\varepsilon^+, 0) &= \tau_i - a_i((1 - q^+)c + qd - \tau^+) - a_i 0 \\ &= \tau_i - a_i((1 - 1)c + d - d) \\ &= \tau_i\end{aligned}$$

which is equal to $(m_1^k)^+$,

$$\begin{aligned}\rho_k(x_\varepsilon^+, c) &= \tau_k - a_k((1 - q^+)c + qd - \tau^+) - a_k 0 \\ &= \tau_k - a_k((1 - 1)c + d - d) - a_k c \\ &= \tau_k - a_k c\end{aligned}$$

which is equal to $(m_2^i)^+ = m_1^k$,

$$\begin{aligned}\rho_k(x_\varepsilon^+, c + d) &= \tau_k - a_k((1 - q^+)c + qd - \tau^+) - a_k(c + d) \\ &= \tau_k - a_k((1 - 1)c + d - d) - a_k(c + d) \\ &= \tau_k - a_k(c + d)\end{aligned}$$

which is equal to $(m_3^i)^+ = m_2^i$,

$$\begin{aligned}\rho_k(x_\varepsilon^+, 2c + d) &= \tau_k - a_k((1 - q^+)c + qd - \tau^+) - a_k(2c + d) \\ &= \tau_k - a_k((1 - 1)c + d - d) - a_k(2c + d) \\ &= \tau_k - a_k(2c + d)\end{aligned}$$

which is equal to $(m_4^i)^+ = m_3^i$,

$$\begin{aligned}\rho_i(x_\varepsilon^+, 2c + 2d) &= \tau_i - a_i((1 - q^+)c + qd - \tau^+) - a_i(2c + 2d) \\ &= \tau_i - a_i((1 - 1)c + d - d) - a_i(2c + 2d) \\ &= \tau_i - a_i(2c + 2d)\end{aligned}$$

which is equal to $(m_5^i)^+ = m_4^i$. Therefore, by recalling the definition $\mathcal{M}_6 = \{x_\varepsilon \in \mathcal{X}_\varepsilon : p=5, q=1, m_1^i - \rho_i(x_\varepsilon, 0) = 0, m_2^i - \rho_i(x_\varepsilon, c) = 0, m_3^i - \rho_k(x_\varepsilon, c+d) = 0, m_4^i - \rho_k(x_\varepsilon, 2c+d) = 0, m_5^i - \rho_i(x_\varepsilon, 2c+2d) = 0\}$, we have $G_{\varepsilon_5}(\mathcal{M}_5 \cap D_\varepsilon) \subset \mathcal{M}_6$ for each $x_\varepsilon \in D_{\varepsilon_5}$.

- if $\phi(0, 0) \in \mathcal{M}_6 \cap D_\varepsilon$, the solution jumps according to $x_\varepsilon^+ = G_{\varepsilon_6}(x_\varepsilon)$. The timer τ resets according to $\tau^+ = c$ while $q^+ = 0$ and $p^+ = 0$. Therefore, by recalling the definition $\mathcal{M}_1 = \{x_\varepsilon \in \mathcal{X}_\varepsilon : p=0, q=0\}$, we have $G_{\varepsilon_5}(\mathcal{M}_6 \cap D_\varepsilon) \subset \mathcal{M}_1$ for each $x_\varepsilon \in D_{\varepsilon_6}$.

□

Lemma 4.4. *Let constants $d \geq c > 0$ be given. For each maximal solution ϕ to \mathcal{H}_ε , there exists $T^* \geq 0$ such that $\phi(t, j) \in \mathcal{M}$ for any $(t, j) \in \text{dom } \phi$ with $t + j \geq T^*$.*

Proof. Pick a solution $\phi \in \mathcal{S}_{\mathcal{H}_\varepsilon}$ with initial condition $\phi(0, 0) \in C_\varepsilon \cup D_\varepsilon$. Since, the flow map F_ε enforces $\dot{p} = 0$, the p component of ϕ remains constant during flows. At jumps, namely, when $\phi(t, j) \in D_\varepsilon$, since for each $\ell \in \{1, 2, 3, 4, 5\}$, G_{ε_ℓ} enforces that $p^+ = p+1$, the evolution of p is monotonically increasing in $\{0, 1, 2, 3, 4, 5\}$ until $p = 5$, from where G_6 resets p to 0. In fact, when the solution ϕ jumps according to G_{ε_6} , we have that $p^+ = 0$ and $q^+ = 0$ resulting in a value for x_ε after the jump that is in \mathcal{M}_1 . Now, due to the monotonic behavior of p and the completeness of solutions to \mathcal{H}_ε given by Lemma 4.2, there exists $(t, j) \in \text{dom } \phi$ such that $\phi(t, j) = G_{\varepsilon_6}(\phi(t, j))$. Given such (t, j) , let $T^* = t + j$. Then, given that $G_{\varepsilon_6}(\phi(t, j)) \subset \mathcal{M}_1$ and the forward invariance of \mathcal{M} given by Lemma 4.3, we have that $\phi(t, j) \in \mathcal{M}$ for each $(t, j) \in \text{dom } \phi$ such that $t + j \geq T^*$. □

In our main result, which is presented in the next section, we show asymptotic attractivity of the synchronization set \mathcal{A}_ε via a Lyapunov analysis on solutions from the initialization set \mathcal{M} .

5 Main Results

In this section, we present our main result showing asymptotic attractivity of the synchronization set \mathcal{A}_ε in (24) for \mathcal{H}_ε . To show this, we present a Lyapunov analysis along solutions to \mathcal{H} starting from the set \mathcal{M} . We remind the reader that \mathcal{M} is the set that denotes valid initialization values of the memory state vectors m^i and m^k for which the update laws $K_{\hat{o}}$ and K_a give values to correct the clock rate and offset. To this end, consider the Lyapunov function candidate

$$V(x_\varepsilon) = \varepsilon^\top \exp(A_f^\top r(\tau, p, q)) P \exp(A_f r(\tau, p, q)) \varepsilon \quad (28)$$

where $P = P^\top \succ 0$, A_f is as given in (20), $r(\tau, p, q) := \tau h(q) + d(5 - p)$ and $h(q) := 1 + c^{-1}(1 - q)(d - c)$ are defined for each $x_\varepsilon \in C_\varepsilon \cup D_\varepsilon$. Note that there exist two positive scalars, α_1 and α_2 , such that

$$\alpha_1 |x_\varepsilon|_{\mathcal{A}_\varepsilon}^2 \leq V(x_\varepsilon) \leq \alpha_2 |x_\varepsilon|_{\mathcal{A}_\varepsilon}^2 \quad \forall x_\varepsilon \in C_\varepsilon \cup D_\varepsilon \quad (29)$$

The function V satisfies the following infinitesimal properties.

Lemma 5.1. *Let the hybrid system \mathcal{H}_ε be given as in (23). For each point $x_\varepsilon \in C_\varepsilon$, one has*

$$\langle \nabla V(x_\varepsilon), F_\varepsilon(x_\varepsilon) \rangle \leq \begin{cases} 0 & \text{if } x_\varepsilon \in C_{\varepsilon_2} \\ \frac{\gamma}{\alpha_2} V(x_\varepsilon) & \text{if } x_\varepsilon \in C_{\varepsilon_1} \end{cases} \quad (30)$$

where

$$\alpha_2 = \lambda_{\max}_{\nu \in \mathcal{Q}, \sigma \in \mathcal{P}} \left(\exp((\nu h(\nu) + d(5 - \sigma)) A_f^\top) P \exp((\nu h(\nu) + d(5 - \sigma)) A_f) \right) \quad (31)$$

$$\gamma = |\alpha| \max \left\{ \frac{p_{11}\epsilon}{2}, \beta + \frac{p_{11}}{2\epsilon} \right\} \quad (32)$$

$\alpha = \frac{2(c-d)}{c}$, $\epsilon > 0$, $\beta = p_{11}6d - p_{12}$, and p_{11} and p_{12} come from $P = \begin{bmatrix} p_{11} & p_{12} \\ p_{21} & p_{22} \end{bmatrix} \succ 0$.

Proof. Before calculating $\langle \nabla V(x_\varepsilon), F_\varepsilon(x_\varepsilon) \rangle$, observe that the full expression of V is given by

$$\begin{aligned}
V(x_\varepsilon) &= \begin{bmatrix} \varepsilon_\tau \\ \varepsilon_a \end{bmatrix}^\top \exp(A_f^\top r(\tau, p, q)) \begin{bmatrix} p_{11} & p_{12} \\ p_{21} & p_{22} \end{bmatrix} \exp(A_f r(\tau, p, q)) \begin{bmatrix} \varepsilon_\tau \\ \varepsilon_a \end{bmatrix} \\
&= \begin{bmatrix} \varepsilon_\tau \\ \varepsilon_a \end{bmatrix}^\top \begin{bmatrix} 1 & 0 \\ r(\tau, p, q) & 1 \end{bmatrix} \begin{bmatrix} p_{11} & p_{12} \\ p_{21} & p_{22} \end{bmatrix} \begin{bmatrix} 1 & r(\tau, p, q) \\ 0 & 1 \end{bmatrix} \begin{bmatrix} \varepsilon_\tau \\ \varepsilon_a \end{bmatrix} \\
&= \begin{bmatrix} \varepsilon_\tau + \varepsilon_a r(\tau, p, q) \\ \varepsilon_a \end{bmatrix}^\top \begin{bmatrix} p_{11} & p_{12} \\ p_{21} & p_{22} \end{bmatrix} \begin{bmatrix} \varepsilon_\tau + \varepsilon_a r(\tau, p, q) \\ \varepsilon_a \end{bmatrix} \\
&= \begin{bmatrix} \varepsilon_\tau + \varepsilon_a r(\tau, p, q) \\ \varepsilon_a \end{bmatrix}^\top \begin{bmatrix} p_{11}(\varepsilon_\tau + \varepsilon_a r(\tau, p, q)) + p_{12}\varepsilon_a \\ p_{21}(\varepsilon_\tau + \varepsilon_a r(\tau, p, q)) + p_{22}\varepsilon_a \end{bmatrix} \\
&= (\varepsilon_\tau + \varepsilon_a r(\tau, p, q))(p_{11}(\varepsilon_\tau + \varepsilon_a r(\tau, p, q)) + p_{12}\varepsilon_a) + \varepsilon_a(p_{21}(\varepsilon_\tau + \varepsilon_a r(\tau, p, q)) + p_{22}\varepsilon_a) \\
&= p_{11}(\varepsilon_\tau + \varepsilon_a r(\tau, p, q))^2 + p_{12}\varepsilon_a(\varepsilon_\tau + \varepsilon_a r(\tau, p, q)) + p_{21}\varepsilon_a(\varepsilon_\tau + \varepsilon_a r(\tau, p, q)) + p_{22}\varepsilon_a^2
\end{aligned} \tag{33}$$

then since $p_{12} = p_{21}$

$$V(x_\varepsilon) = p_{11}(\varepsilon_\tau + \varepsilon_a r(\tau, p, q))^2 + 2p_{12}\varepsilon_a(\varepsilon_\tau + \varepsilon_a r(\tau, p, q)) + p_{22}\varepsilon_a^2 \tag{34}$$

In calculating $\langle \nabla V(x_\varepsilon), F_\varepsilon(x_\varepsilon) \rangle$, one has

$$\begin{aligned}
\langle \nabla V(x_\varepsilon), F_\varepsilon(x_\varepsilon) \rangle &= [\nabla_{\varepsilon_\tau} V(x_\varepsilon) \quad \nabla_{\varepsilon_a} V(x_\varepsilon) \quad \nabla_\tau V(x_\varepsilon) \quad \nabla_p V(x_\varepsilon) \quad \nabla_q V(x_\varepsilon)] \begin{bmatrix} \varepsilon_a \\ 0 \\ -1 \\ 0 \\ 0 \end{bmatrix} \\
&= \nabla_{\varepsilon_\tau} V(x_\varepsilon)\varepsilon_a - \nabla_\tau V(x_\varepsilon)
\end{aligned} \tag{35}$$

where

$$\begin{aligned}
\nabla_{\varepsilon_\tau} V(x_\varepsilon) &= 2p_{11}(\varepsilon_\tau + \varepsilon_a r(\tau, p, q)) + 2p_{12}\varepsilon_a \\
\nabla_\tau V(x_\varepsilon) &= 2p_{11}\varepsilon_a \nabla_\tau r(\tau, p, q)(\varepsilon_\tau + \varepsilon_a r(\tau, p, q)) + 2p_{12}\varepsilon_a^2 \nabla_\tau r(\tau, p, q)
\end{aligned} \tag{36}$$

Substituting (36) into (35), we obtain

$$\begin{aligned}
\langle \nabla V(x_\varepsilon), F_\varepsilon(x_\varepsilon) \rangle &= \left(2p_{11}(\varepsilon_\tau + \varepsilon_a r(\tau, p, q)) + 2p_{12}\varepsilon_a \right) \varepsilon_a \\
&\quad - 2p_{11}\varepsilon_a \nabla_\tau r(\tau, p, q)(\varepsilon_\tau + \varepsilon_a r(\tau, p, q)) - 2p_{12}\varepsilon_a^2 \nabla_\tau r(\tau, p, q) \\
&= 2p_{11}\varepsilon_a(\varepsilon_\tau + \varepsilon_a r(\tau, p, q)) + 2p_{12}\varepsilon_a^2 \\
&\quad - 2p_{11}\varepsilon_a \nabla_\tau r(\tau, p, q)(\varepsilon_\tau + \varepsilon_a r(\tau, p, q)) - 2p_{12}\varepsilon_a^2 \nabla_\tau r(\tau, p, q) \\
&= 2p_{11}\varepsilon_a(\varepsilon_\tau + \varepsilon_a r(\tau, p, q))(1 - \nabla_\tau r(\tau, p, q)) + 2p_{12}\varepsilon_a^2(1 - \nabla_\tau r(\tau, p, q)) \\
&= (2p_{11}\varepsilon_a(\varepsilon_\tau + \varepsilon_a r(\tau, p, q)) + 2p_{12}\varepsilon_a^2)(1 - \nabla_\tau r(\tau, p, q)) \\
&= (2p_{11}(\varepsilon_a \varepsilon_\tau + \varepsilon_a^2 r(\tau, p, q)) + 2p_{12}\varepsilon_a^2)(1 - \nabla_\tau r(\tau, p, q))
\end{aligned}$$

for each $x_\varepsilon \in C_\varepsilon$. Now, with $\nabla_\tau r(\tau, p, q) = \frac{(c-d)(q-1)}{c} + 1$, when $x_\varepsilon \in C_{\varepsilon_2}$ with $q = 1$, $\nabla_\tau r(\tau, p, q) = 1$, thus

$$\langle \nabla V(x_\varepsilon), F_\varepsilon(x_\varepsilon) \rangle = 0$$

When $x_\varepsilon \in C_{\varepsilon_2}$ with $q = 0$, $r(\tau, p, q) = \tau\left(\frac{d-c}{c}+1\right) + d(5-p)$ and $\nabla_\tau r(\tau, p, q) = \frac{d-c}{c} + 1$ one then has

$$\begin{aligned}
\langle \nabla V(x_\varepsilon), F_\varepsilon(x_\varepsilon) \rangle &= \left(2p_{11}\varepsilon_a \varepsilon_\tau + 2p_{11}\varepsilon_a^2 \left(\tau \left(\frac{d-c}{c} + 1 \right) + d(5-p) \right) + 2p_{12}\varepsilon_a^2 \right) \left(\frac{c-d}{c} \right) \\
&= \left(2p_{11}\varepsilon_a \varepsilon_\tau + 2p_{11}\varepsilon_a^2 \left(\tau \left(\frac{d-c}{c} \right) + \tau + d(5-p) \right) + 2p_{12}\varepsilon_a^2 \right) \left(\frac{c-d}{c} \right) \\
&= \left(\frac{c-d}{c} \right) 2p_{11}\varepsilon_a \varepsilon_\tau + \left(\frac{c-d}{c} \right) 2p_{11}\varepsilon_a^2 \left(\tau \left(\frac{d-c}{c} \right) + \tau + d(5-p) \right) \\
&\quad + \left(\frac{c-d}{c} \right) 2p_{12}\varepsilon_a^2 \\
&= \left(\frac{2(c-d)}{c} \right) p_{11}\varepsilon_a \varepsilon_\tau + \left(\frac{2(c-d)}{c} \right) p_{11}\varepsilon_a^2 \left(\tau \left(\frac{d-c}{c} \right) + \tau + d(5-p) \right) \\
&\quad + \left(\frac{2(c-d)}{c} \right) p_{12}\varepsilon_a^2
\end{aligned}$$

Let $\alpha = \frac{2(c-d)}{c}$, then since, $0 < c \leq d$ we have that $\alpha \leq 0$

$$\langle \nabla V(x_\varepsilon), F_\varepsilon(x_\varepsilon) \rangle = -|\alpha|p_{11}\varepsilon_a \varepsilon_\tau - |\alpha|p_{11}\varepsilon_a^2 \left(\tau \left(\frac{d-c}{c} \right) + \tau + d(5-p) \right) - |\alpha|p_{12}\varepsilon_a^2$$

Then, recognizing that $\tau \in [0, c]$ when $x_\varepsilon \in C_{\varepsilon_2}$ then we have that $\tau \leq c$,

which due to the fact that $p_{11} > 0$ and $p \in \mathcal{P} = \{0, 1, 2, 3, 4, 5\}$ leading to

$$\begin{aligned} \langle \nabla V(x_\varepsilon), F_\varepsilon(x_\varepsilon) \rangle &\leq -|\alpha|p_{11}\varepsilon_a\varepsilon_\tau + |\alpha|p_{11}\left(c\left(\frac{d-c}{c}\right) + c + d(5-p)\right)\varepsilon_a^2 - |\alpha|p_{12}\varepsilon_a^2 \\ &\leq -|\alpha|p_{11}\varepsilon_a\varepsilon_\tau + |\alpha|p_{11}\left((d-c) + c + d(5-p)\right)\varepsilon_a^2 - |\alpha|p_{12}\varepsilon_a^2 \\ &\leq -|\alpha|p_{11}\varepsilon_a\varepsilon_\tau + |\alpha|p_{11}d(6-p)\varepsilon_a^2 - |\alpha|p_{12}\varepsilon_a^2 \end{aligned}$$

for each $x_\varepsilon \in C_{\varepsilon_2}$. We can upper bound the quantity $6-p$ by noting that $p \in \mathcal{P} = \{0, 1, 2, 3, 4, 5\}$. Thus, we have that $6-p \leq 6$ for each $p \in \mathcal{P}$, leading to

$$\langle \nabla V(x_\varepsilon), F_\varepsilon(x_\varepsilon) \rangle \leq -|\alpha|p_{11}\varepsilon_a\varepsilon_\tau + |\alpha|(p_{11}6d - p_{12})\varepsilon_a^2$$

Now, with $\beta = p_{11}6d - p_{12}$. Then, we obtain

$$\langle \nabla V(x_\varepsilon), F_\varepsilon(x_\varepsilon) \rangle \leq |\alpha|p_{11}|\varepsilon_a||\varepsilon_\tau| + |\alpha|\beta\varepsilon_a^2 \quad \forall x_\varepsilon \in C_{\varepsilon_2} \quad (37)$$

Then, through an application of Young's inequality one has

$$\begin{aligned} \langle \nabla V(x_\varepsilon), F_\varepsilon(x_\varepsilon) \rangle &\leq |\alpha|p_{11}\left(\frac{1}{2\epsilon}\varepsilon_a^2 + \frac{\epsilon}{2}\varepsilon_\tau^2\right) + |\alpha|\beta\varepsilon_a^2 \\ &\leq \frac{|\alpha|p_{11}}{2\epsilon}\varepsilon_a^2 + |\alpha|\beta\varepsilon_a^2 + \frac{|\alpha|p_{11}\epsilon}{2}\varepsilon_\tau^2 \\ &\leq \frac{|\alpha|p_{11}\epsilon}{2}\varepsilon_\tau^2 + |\alpha|\left(\beta + \frac{p_{11}}{2\epsilon}\right)\varepsilon_a^2 \\ &\leq \gamma(\varepsilon_\tau^2 + \varepsilon_a^2) \\ &\leq \gamma\varepsilon^\top\varepsilon \end{aligned}$$

for each $x_\varepsilon \in C_{\varepsilon_2}$. Then, from the definition of V in (28)

$$\begin{aligned} \langle \nabla V(x_\varepsilon), F_\varepsilon(x_\varepsilon) \rangle &\leq \gamma|x_\varepsilon|^2 \\ &\leq \frac{\gamma}{\alpha_2}V(x_\varepsilon) \end{aligned}$$

for each $x_\varepsilon \in C_{\varepsilon_2}$ where $\epsilon > 0$, α_2 and γ are positive constants given in (31) and (32), respectively. \square

Lemma 5.2. *Let the hybrid system \mathcal{H}_ε in (23) with constants $d \geq c > 0$ be given. If there exist a constant $\mu > 0$ and a positive definite symmetric matrix P such that*

$$A_g^\top \exp(6dA_f^\top)P \exp(6dA_f)A_g - P \prec 0 \quad (38)$$

where $A_g = \begin{bmatrix} 0 & \gamma_1 \\ 0 & 1-\mu\gamma_2 \end{bmatrix}$ and A_f is as given in (20) with $\gamma_1 = \frac{1}{2}(3c + 4d)$ and $\gamma_2 = 2c + 2d$ then, for each $x_\varepsilon \in \mathcal{M} \cap D_\varepsilon$,

$$V(G_\ell(x_\varepsilon)) - V(x_\varepsilon) \leq 0$$

for each $\ell \in \{1, 2, 3, 4, 5\}$, and ⁵

$$V(G_6(x_\varepsilon)) - V(x_\varepsilon) \leq -\sigma \varepsilon^\top \varepsilon$$

where

$$\sigma \in \left(0, -\lambda_{\min} \left(A_g^\top \exp((6d)A_f^\top) P \exp((6d)A_f) A_g - P \right) \right) \quad (39)$$

Proof. For every $g \in G_\varepsilon(x_\varepsilon)$, the state τ is reset to a point in the set $\{c, d\}$. Moreover, for each $x_\varepsilon \in D_\varepsilon$, $\tau = 0$. Hence, when $x_\varepsilon \in D_{\varepsilon_1} \cap \mathcal{M}_1$, we have that $\tau = 0$, $q = 0$, and $p = 0$, leading to

$$\begin{aligned} V(G_{\varepsilon_1}(x_\varepsilon)) - V(x_\varepsilon) &= \varepsilon^\top \exp(A_f^\top(d + d(5-1))) P \exp(A_f(d + d(5-1))) \varepsilon \\ &\quad - \varepsilon^\top \exp(A_f^\top(0 + d(5-0))) P \exp(A_f(0 + d(5-0))) \varepsilon \\ &= \varepsilon^\top \exp(A_f^\top(5d)) P \exp(A_f(5d)) \varepsilon \\ &\quad - \varepsilon^\top \exp(A_f^\top(5d)) P \exp(A_f(5d)) \varepsilon \\ &= 0 \end{aligned}$$

When $x_\varepsilon \in D_{\varepsilon_2} \cap \mathcal{M}_2$, we have that $\tau = 0$, $q = 1$, and $p = 1$, leading to

$$\begin{aligned} V(G_{\varepsilon_2}(x_\varepsilon)) - V(x_\varepsilon) &= \varepsilon^\top \exp(A_f^\top(c(1 + c^{-1}(d - c)) + d(5-2))) P \exp(A_f(c(1 \\ &\quad + c^{-1}(d - c)) + d(5-2))) \varepsilon \\ &\quad - \varepsilon^\top \exp(A_f^\top(0 + d(5-1))) P \exp(A_f(0 + d(5-1))) \varepsilon \\ &= \varepsilon^\top \exp(A_f^\top(d + 3d)) P \exp(A_f(d + 3d)) \varepsilon \\ &\quad - \varepsilon^\top \exp(A_f^\top(4d)) P \exp(A_f(4d)) \varepsilon \\ &= 0 \end{aligned}$$

⁵Observe that $\varepsilon^+ = A_g \varepsilon$ is the matrix representation of the jump map G_6 for which ε is reset to when $x_\varepsilon \in \mathcal{M}_6 \cap D_\varepsilon$.

When $x_\varepsilon \in D_{\varepsilon_3} \cap \mathcal{M}_3$, we have that $\tau = 0$, $q = 0$, and $p = 2$, leading to

$$\begin{aligned}
V(G_{\varepsilon_3}(x_\varepsilon)) - V(x_\varepsilon) &= \varepsilon^\top \exp(A_f^\top(d + d(5-3)))P \exp(A_f(d + d(5-3)))\varepsilon \\
&\quad - \varepsilon^\top \exp(A_f^\top(0 + d(5-2)))P \exp(A_f(0 + d(5-2)))\varepsilon \\
&= \varepsilon^\top \exp(A_f^\top(3d))P \exp(A_f(3d))\varepsilon \\
&\quad - \varepsilon^\top \exp(A_f^\top(3d))P \exp(A_f(3d))\varepsilon \\
&= 0
\end{aligned}$$

When $x_\varepsilon \in D_{\varepsilon_4} \cap \mathcal{M}_4$, we have that $\tau = 0$, $q = 1$, and $p = 3$, leading to

$$\begin{aligned}
V(G_{\varepsilon_4}(x_\varepsilon)) - V(x_\varepsilon) &= \varepsilon^\top \exp(A_f^\top(c(1 + c^{-1}(d - c)) + d(5-4)))P \exp(A_f(c(1 \\
&\quad + c^{-1}(d - c)) + d(5-4)))\varepsilon \\
&\quad - \varepsilon^\top \exp(A_f^\top(0 + d(5-3)))P \exp(A_f(0 + d(5-3)))\varepsilon \\
&= \varepsilon^\top \exp(A_f^\top(d + d))P \exp(A_f(d + d))\varepsilon \\
&\quad - \varepsilon^\top \exp(A_f^\top(2d))P \exp(A_f(2d))\varepsilon \\
&= 0
\end{aligned}$$

When $x_\varepsilon \in D_{\varepsilon_5} \cap \mathcal{M}_5$, we have that $\tau = 0$, $q = 0$, and $p = 4$, leading to

$$\begin{aligned}
V(G_{\varepsilon_5}(x_\varepsilon)) - V(x_\varepsilon) &= \varepsilon^\top \exp(A_f^\top(d + d(5-5)))P \exp(A_f(d + d(5-5)))\varepsilon \\
&\quad - \varepsilon^\top \exp(A_f^\top(0 + d(5-4)))P \exp(A_f(0 + d(5-4)))\varepsilon \\
&= \varepsilon^\top \exp(A_f^\top(d))P \exp(A_f(d))\varepsilon \\
&\quad - \varepsilon^\top \exp(A_f^\top(d))P \exp(A_f(d))\varepsilon \\
&= 0
\end{aligned}$$

When $x_\varepsilon \in D_{\varepsilon_6} \cap \mathcal{M}_6$, we have that $\tau = 0$, $q = 1$, and $p = 5$. For resets according to G_{ε_6} , one has

$$\begin{aligned}
V(G_{\varepsilon_6}(x_\varepsilon)) - V(x_\varepsilon) &= \\
&\left[\varepsilon + \begin{bmatrix} K_{\bar{\delta}}(m^i) \\ -K_a(m^i, \tau_k) \end{bmatrix} \right]^\top \exp(A_f^\top(c(1+c^{-1}(d-c))+d(5-0)))P \exp(A_f(c(1 \\
&\quad +c^{-1}(d-c))+d(5-0))) \left[\varepsilon + \begin{bmatrix} K_{\bar{\delta}}(m^i) \\ -K_a(m^i, \tau_k) \end{bmatrix} \right] \\
&\quad - \varepsilon^\top \exp(A_f^\top(0 + d(0)))P(A_f^\top(0 + d(0)))\varepsilon \\
&= \left[\varepsilon + \begin{bmatrix} K_{\bar{\delta}}(m^i) \\ -K_a(m^i, \tau_k) \end{bmatrix} \right]^\top \exp(A_f^\top(6d))P \exp(A_f(6d)) \left[\varepsilon + \begin{bmatrix} K_{\bar{\delta}}(m^i) \\ -K_a(m^i, \tau_k) \end{bmatrix} \right] \\
&\quad - \varepsilon^\top P \varepsilon
\end{aligned}$$

Now, with $x_\varepsilon \in D_{\varepsilon_6} \cap \mathcal{M}_6$, which implies that $p = 5$, $q = 1$, and $\tau = 0$, one has that for jumps with resets according to $G_{\varepsilon_6}(x_\varepsilon)$, the feedback laws $K_{\bar{\delta}}$ and K_a applied to τ_k and a_k , respectively, give

$$\begin{aligned}
K_{\bar{\delta}}(m^i) &= \frac{1}{2}(m_4^i - m_5^i - m_2^i + m_3^i) \\
&= \frac{1}{2} \left(\left((\tau_k - a_k(2c + 2d)) - (\tau_i - a_i(2c + 3d)) \right) \right. \\
&\quad \left. - \left((\tau_i - a_i(c + d)) - (\tau_k - a_k(c + 2d)) \right) \right) \\
&= \frac{1}{2} \left(2(\tau_k - \tau_i) + a_i(3c + 4d) - a_k(3c + 4d) \right) \\
&= (\tau_k - \tau_i) + \frac{1}{2}(a_i - a_k)(3c + 4d) \\
&= -\varepsilon_\tau + \gamma_1 \varepsilon_a \\
K_a(m^i, \tau_k) &= \mu \left((m_1^i - m_5^i) - (\tau_k - m_4^i) \right) \\
&= \mu \left((\tau_i - a_i(d) - (\tau_i - a_i(2c + 3d))) \right. \\
&\quad \left. - (\tau_k - (\tau_k - a_k(2c + 2d))) \right) \\
&= \mu \left((a_i(2c + 3d) + a_i(d)) - (a_k(2c + 2d)) \right) \\
&= \mu(a_i - a_k)(2c + 2d) \\
&= \mu\gamma_2 \varepsilon_a
\end{aligned}$$

where $\gamma_1 = \frac{3c+4d}{2}$ and $\gamma_2 = 2(c + d)$. Using the expressions for $K_{\bar{\delta}}(m^i)$ and $K_a(m^i, \tau_k)$, it follows that

$$\begin{aligned}
V(G_{\varepsilon_6}(x_\varepsilon)) - V(x_\varepsilon) &= \left[\varepsilon + \begin{bmatrix} K_{\bar{\delta}}(m^i) \\ -K_a(m^i, \tau_k) \end{bmatrix} \right]^\top \exp(6dA_f^\top) P \exp(6dA_f) \left[\varepsilon + \begin{bmatrix} K_{\bar{\delta}}(m^i) \\ -K_a(m^i, \tau_k) \end{bmatrix} \right] \\
&\quad - \varepsilon^\top P \varepsilon \\
&= \begin{bmatrix} \varepsilon_\tau - \varepsilon_\tau + \gamma_1 \varepsilon_a \\ \varepsilon_a - \mu\gamma_2 \varepsilon_a \end{bmatrix}^\top \exp(6dA_f^\top) P \exp(6dA_f) \begin{bmatrix} \varepsilon_\tau - \varepsilon_\tau + \gamma_1 \varepsilon_a \\ \varepsilon_a - \mu\gamma_2 \varepsilon_a \end{bmatrix} \\
&\quad - \varepsilon^\top P \varepsilon \\
&= \varepsilon \begin{bmatrix} 0 & \gamma_1 \\ 0 & 1 - \mu\gamma_2 \end{bmatrix}^\top \exp(6dA_f^\top) P \exp(6dA_f) \begin{bmatrix} 0 & \gamma_1 \\ 0 & 1 - \mu\gamma_2 \end{bmatrix} \varepsilon - \varepsilon^\top P \varepsilon \\
&= \varepsilon^\top A_g^\top \exp(6dA_f^\top) P \exp(6dA_f) A_g \varepsilon - \varepsilon^\top P \varepsilon \\
&= \varepsilon^\top \left(A_g^\top \exp(6dA_f^\top) P \exp(6dA_f) A_g - P \right) \varepsilon
\end{aligned}$$

for each $x_\varepsilon \in D_{\varepsilon_6} \cap \mathcal{M}_6$. Then, by continuity of condition (38), there exists

σ as in (39) such that

$$V(G_{\varepsilon_6}) - V(x_\varepsilon) \leq -\sigma \varepsilon^\top \varepsilon$$

for each $x_\varepsilon \in D_{\varepsilon_6} \cap \mathcal{M}_6$. \square

Remark 5.3. *Observe that condition (38) may be difficult to satisfy numerically as it may not be convex in μ and P . The authors in [25] utilize a polytopic embedding strategy to arrive at a linear matrix inequality in which one needs to find some matrices X_i such that the exponential matrix is an element in the convex hull of the X_i matrices. Such an algorithm can be adapted to our setting.*

Theorem 5.4. *Let the hybrid system \mathcal{H}_ε in (23) with constants $d \geq c > 0$ be given. If there exist a constant $\mu > 0$ and a positive definite symmetric matrix P such that (38) holds with $\gamma_1 = \frac{3c+4d}{2}$ and $\gamma_2 = 2(c+d)$, and σ as in (39) such that*

$$\eta^{\frac{1}{6}} \rho < 1 \quad (40)$$

with $\eta = |1 - \frac{\sigma}{\alpha_2}|$ and $\rho = \exp\left(\frac{\gamma c}{2\alpha_2}\right)$ holds, where α_2 and γ are as given in (32) and (32), respectively, then \mathcal{A}_ε is globally attractive for \mathcal{H}_ε . Moreover, every maximal solution ϕ_ε to \mathcal{H}_ε with $\phi(0,0) \in (C_\varepsilon \cup D_\varepsilon) \cap \mathcal{M}$, satisfies

$$|\phi(t,j)|_{\mathcal{A}_\varepsilon} \leq \sqrt{\frac{\alpha_2}{\alpha_1} \eta^{\frac{j}{6}} \rho^j \exp\left(\frac{\gamma c}{\alpha_2}\right)} |\phi(0,0)|_{\mathcal{A}_\varepsilon} \quad \forall (t,j) \in \text{dom } \phi \quad (41)$$

where

$$\alpha_1 = \lambda_{\min}_{\nu \in \mathcal{Q}, \sigma \in \mathcal{P}} \left(\exp((\nu h(\nu) + d(5-\sigma))A_f^\top) P \exp((\nu h(\nu) + d(5-\sigma))A_f) \right)$$

and, consequently, $\lim_{t+j \rightarrow \infty} |\phi(t,j)|_{\mathcal{A}_\varepsilon} = 0$.

Proof. Pick a maximal solution with initial condition $\phi_\varepsilon(0,0) \in (C_\varepsilon \cup D_\varepsilon) \cap \mathcal{M}$. Recall the function V in (29), from the proof of Lemma 5.2 we have that

$$V(G_{\varepsilon_6}(x_\varepsilon)) - V(x_\varepsilon) \leq -\sigma \varepsilon^\top \varepsilon \quad \forall x_\varepsilon \in D_{\varepsilon_6} \cap \mathcal{M} \quad (42)$$

and from the definition of V in (29), there exists a positive scalar α_2 as in (31) such that

$$V(x_\varepsilon) \leq \alpha_2 |x_\varepsilon|_{\mathcal{A}_\varepsilon}^2$$

rearranging terms one then has

$$-|x_\varepsilon|_{\mathcal{A}_\varepsilon}^2 \leq -\frac{1}{\alpha_2}V(x_\varepsilon)$$

Then, by making the appropriate substitutions in (42), since $\varepsilon^\top \varepsilon = |x_\varepsilon|_{\mathcal{A}_\varepsilon}^2$ one has

$$\begin{aligned} V(G_{\varepsilon_6}(x_\varepsilon)) - V(x_\varepsilon) &\leq -\frac{\sigma}{\alpha_2}V(x_\varepsilon) \\ V(G_{\varepsilon_6}(x_\varepsilon)) &\leq \left|1 - \frac{\sigma}{\alpha_2}\right|V(x_\varepsilon) \end{aligned}$$

From Lemma 5.1 we have that for each $x_\varepsilon \in C_\varepsilon$,

$$\langle \nabla V(x_\varepsilon), F_\varepsilon(x_\varepsilon) \rangle \leq \begin{cases} 0 & \text{if } x_\varepsilon \in C_{\varepsilon_2} \\ \frac{\gamma}{\alpha_2}V(x_\varepsilon) & \text{if } x_\varepsilon \in C_{\varepsilon_1} \end{cases} \quad (43)$$

and from Lemma 5.2 we have that for each $x_\varepsilon \in D_\varepsilon \cap \mathcal{M}$,

$$V(G_{\varepsilon_\ell}(x_\varepsilon)) \leq \begin{cases} V(x_\varepsilon) & \text{if } \ell \in \{1, 2, 3, 4, 5\} \\ \left(1 - \frac{\sigma}{\alpha_2}\right)V(x_\varepsilon) & \text{if } \ell = 6 \end{cases} \quad (44)$$

Pick a solution ϕ to \mathcal{H}_ε with $\phi_\varepsilon(0, 0) \in C_\varepsilon \cap \mathcal{M}_1$. Then for each $(t, j) \in [0, t_1] \times \{0\}$

$$V(\phi_\varepsilon(t, 0)) \leq \exp\left(\frac{\gamma}{\alpha_2}(t_1 - 0)\right)V(\phi_\varepsilon(0, 0))$$

At $(t_1, 1)$, following a reset according to G_{ε_1} one has

$$V(\phi_\varepsilon(t_1, 1)) \leq V(\phi_\varepsilon(t_1, 0))$$

Then, since $\phi_q(t_1, 1) = 1$ for each $(t, j) \in [t_1, t_2] \times \{1\}$, we obtain

$$V(\phi_\varepsilon(t, 1)) \leq V(\phi_\varepsilon(t_1, 1))$$

At $(t_2, 2)$, following a reset according to G_{ε_2} one has

$$V(\phi_\varepsilon(t_2, 2)) \leq V(\phi_\varepsilon(t_2, 1))$$

Then since $\phi_q(t_2, 2) = 0$ for each $(t, j) \in [t_2, t_3] \times \{2\}$, we obtain

$$V(\phi_\varepsilon(t, 2)) \leq \exp\left(\frac{\gamma}{\alpha_2}(t_3 - t_2)\right)V(\phi_\varepsilon(t_2, 2))$$

At $(t_3, 3)$, following a reset according to G_{ε_3} one has

$$V(\phi_\varepsilon(t_3, 3)) \leq V(\phi_\varepsilon(t_3, 3))$$

Then since $\phi_q(t_3, 3) = 1$ for each $(t, j) \in [t_3, t_4] \times \{3\}$, we obtain

$$V(\phi_\varepsilon(t, 3)) \leq V(\phi_\varepsilon(t_3, 2))$$

At $(t_4, 4)$ following a reset according to G_{ε_4} one has

$$V(\phi_\varepsilon(t_4, 4)) \leq V(\phi_\varepsilon(t_4, 3))$$

Then since $\phi_q(t_4, 4) = 0$ for each $(t, j) \in [t_4, t_5] \times \{4\}$, we obtain

$$V(\phi_\varepsilon(t, 4)) \leq \exp\left(\frac{\gamma}{\alpha_2}(t_5 - t_4)\right)V(\phi_\varepsilon(t_4, 4))$$

At $(t_5, 5)$, following a reset according to G_{ε_5} one has

$$V(\phi_\varepsilon(t_5, 5)) \leq V(\phi_\varepsilon(t_5, 4))$$

then since $\phi_q(t_5, 5) = 1$ for each $(t, j) \in [t_5, t_6] \times \{5\}$, we obtain

$$V(\phi_\varepsilon(t, 5)) \leq V(\phi_\varepsilon(t_5, 5))$$

At $(t_6, 6)$, following a reset according to G_{ε_6} one has

$$V(\phi_\varepsilon(t_6, 6)) \leq \left|1 - \frac{\sigma}{\alpha_2}\right|V(\phi_\varepsilon(t_6, 5))$$

Making the appropriate substitutions one has

$$V(\phi_\varepsilon(t_6, 6)) \leq \left|1 - \frac{\sigma}{\alpha_2}\right| \exp\left(\frac{\gamma}{\alpha_2}(t_5 - t_4)\right) \exp\left(\frac{\gamma}{\alpha_2}(t_3 - t_2)\right) \exp\left(\frac{\gamma}{\alpha_2}(t_1 - 0)\right)V(\phi_\varepsilon(0, 0))$$

leading to a general bound of the form

$$V(\phi_\varepsilon(t, j)) \leq \left|1 - \frac{\sigma}{\alpha_2}\right|^{\lfloor \frac{j}{6} \rfloor} \left(\prod_{k=0}^{\lfloor \frac{j-1}{2} \rfloor} \exp\left(\frac{\gamma}{\alpha_2}(t_{2k+1} - t_{2k})\right) \right) V(\phi_\varepsilon(0, 0)) \quad (45)$$

However, by noting the bounds in (3) one has that $t_{j+1} - t_j \leq c(j+1)$ for each $j \in \{2i : i \in \mathbb{N}\}, j > 0$, then assuming $\gamma > 0$, the bound in (45) reduces to

$$V(\phi_\varepsilon(t, j)) \leq \left|1 - \frac{\sigma}{\alpha_2}\right|^{\lfloor \frac{j}{6} \rfloor} \left(\prod_{k=0}^{\lfloor \frac{j-1}{2} \rfloor} \exp\left(\frac{\gamma}{\alpha_2}(c(2k+1))\right) \right) V(\phi_\varepsilon(0, 0))$$

$$V(\phi_\varepsilon(t, j)) \leq \left|1 - \frac{\sigma}{\alpha_2}\right|^{\lfloor \frac{j}{6} \rfloor} \left(\exp\left(\frac{\gamma c}{\alpha_2}\right)\right)^{\lceil \frac{j}{2} \rceil} V(\phi_\varepsilon(0, 0))$$

Using the relation $\lceil \frac{j}{2} \rceil = \frac{j}{2} + 1$ we then have

$$V(\phi_\varepsilon(t, j)) \leq \left|1 - \frac{\sigma}{\alpha_2}\right|^{\lfloor \frac{j}{6} \rfloor} \left(\exp\left(\frac{\gamma c}{\alpha_2}\right)\right)^{\frac{j}{2}} \exp\left(\frac{\gamma c}{\alpha_2}\right) V(\phi_\varepsilon(0, 0))$$

Then noting that $\lfloor \frac{j}{6} \rfloor \leq \frac{j}{6}$

$$V(t, j) \leq \left|1 - \frac{\sigma}{\alpha_2}\right|^{\frac{j}{6}} \left(\exp\left(\frac{\gamma c}{2\alpha_2}\right)\right)^j \exp\left(\frac{\gamma c}{\alpha_2}\right) V(0, 0)$$

Then given the definition of V in (29) we have that

$$\alpha_1 |x_\varepsilon|_{\mathcal{A}_\varepsilon}^2 \leq V(\phi_\varepsilon(t, j)) \leq \left|1 - \frac{\sigma}{\alpha_2}\right|^{\frac{j}{6}} \left(\exp\left(\frac{\gamma c}{2\alpha_2}\right)\right)^j \exp\left(\frac{\gamma c}{\alpha_2}\right) V(\phi_\varepsilon(0, 0)) \quad (46)$$

Finally, by leveraging $V(\phi(0, 0)) \leq \alpha_2 |\phi(0, 0)|_{\mathcal{A}_\varepsilon}^2$, we arrive at (41). \square

6 About the Multi-Agent Case

In this section, we present an extension to the proposed algorithm model to capture the scenario of synchronizing multiple networked agents. For such a setting, we consider a network system of n nodes in a leader-follower scenario where there exists a single designated reference node to which all the connected $N = n - 1$ nodes synchronize. To this end, let $\tau_R \in \mathbb{R}$ define the clock of the designated reference node and $\tau_S := (\tau_{S_1}, \tau_{S_2}, \dots, \tau_{S_N}) \in \mathbb{R}^N$ define the clocks of the synchronizing child nodes, where τ_{S_i} is the clock of the i -th child node. Moreover, we let $a_R \in \mathbb{R}$ and $a := (a_1, a_2, \dots, a_N) \in \mathbb{R}^N$ define the skews of the reference clock and synchronizing clocks, respectively, where a_i is the clock skew of the i -th child node. Given the leader-follower architecture to synchronize the nodes, the algorithm in \mathcal{H} is modified such that the algorithm modeled by \mathcal{H} is executed for each synchronizing node. In particular, the algorithm executes the synchronization process given by (P1)-(P6) for the reference node τ_R and the i -th child node τ_{S_i} . Upon completion, the algorithm then executes the same synchronization steps (P1)-(P6) for the reference node and the mod $(i + 1, N)$ -th child node. This procedure is repeated recurrently and cyclically for each pair reference-child node in the network. To enable the modeling of such an algorithm, we define:

- A discrete variable $\ell \in \{1, 2, \dots, N\} =: \mathcal{S}$ that indexes the node to be synchronized. The variable remains constant during flows, namely, $\dot{s} = 0$, and resets to either $s+1$ upon the completion of the synchronization algorithm for $s \in \{1, 2, \dots, n-2\}$ or is reset to 1 when $s = n-1$.
- For each $\ell \in \mathcal{S}$, a timer variable $\tilde{\tau}_\ell \in [0, 3c + 3d]$ to track the execution of the synchronization algorithm for the respective ℓ -th child node, with dynamics

$$\begin{aligned} \dot{\tilde{\tau}}_\ell &= -1 & \tilde{\tau}_\ell &\in [0, 3c + 3d] \\ \tilde{\tau}_\ell^+ &= 3c + 3d & \tilde{\tau}_\ell &= 0 \end{aligned}$$

for each $\ell \in \mathcal{S}$. The value $3c + 3d$ reflects the duration of the synchronization algorithm executed between the reference and the synchronizing node capturing the total time elapsed during message transmission and residence delay.

The state of this multi-agent system is given by

$$\tilde{x} := (\tau_R, \tau_S, a_R, a, \tau, \tilde{\tau}, m^R, m^S, \ell, p, q) \in \tilde{\mathcal{X}}$$

where $\tilde{\tau} := (\tilde{\tau}_1, \tilde{\tau}_2, \dots, \tilde{\tau}_N)$, $m^R = [m_1^R, m_2^R, m_3^R, m_4^R, m_5^R, m_6^R]^\top \in \mathbb{R}^6$, $m^S = [m_1^S, m_2^S, m_3^S, m_4^S, m_5^S, m_6^S]^\top \in \mathbb{R}^6$ and

$$\tilde{\mathcal{X}} := \mathbb{R} \times \mathbb{R}^N \times \mathbb{R} \times \mathbb{R}^N \times [0, d] \times [0, 3c + 3d]^N \times \mathbb{R}^6 \times \mathbb{R}^6 \times \mathcal{S} \times \mathcal{P} \times \mathcal{Q}$$

Then by noting the dynamics of the clocks as given in (1) and those of the timer $\tilde{\tau}$ above, the continuous dynamics of \tilde{x} is given by

$$\dot{\tilde{x}} = (a_R, a, 0, \mathbf{0}_{N \times 1}, -1, -\mathbf{1}_{(N) \times 1}, \mathbf{0}_{6 \times 1}, \mathbf{0}_{6 \times 1}, 0, 0, 0) \quad \tilde{x} \in \tilde{\mathcal{C}} := \tilde{\mathcal{X}}$$

To model the discrete dynamics of the communication and arrival events of the exchanged timing messages, in addition to the subsequent corrections on the clock rate and offset, we consider the jump map $\tilde{G}(\tilde{x}) := \{\tilde{G}^i(\tilde{x}) : \tilde{x} \in \tilde{D}^i, i \in \mathcal{S}\}$ where

$$\tilde{G}^i(\tilde{x}) = \tilde{G}_k^i(\tilde{x}) \quad \text{if } \tilde{x} \in \tilde{D}_k^i$$

and

$$\begin{aligned}
\tilde{G}_1^i(\tilde{x}) &= \begin{bmatrix} \tau_R \\ \tau_S \\ a_R \\ a \\ d \\ \tilde{\tau} \\ [[\tau_R, m_1^R, \dots, m_5^R] m^s]^\top \\ \ell \\ p+1 \\ 1 \end{bmatrix}, & \tilde{G}_2^i(\tilde{x}) &= \begin{bmatrix} \tau_R \\ \tau \\ a_R \\ a \\ c \\ \tilde{\tau} \\ [m^R [\tau_i, m_1^R, \dots, m_5^R]]^\top \\ \ell \\ p+1 \\ 0 \end{bmatrix}, \\
\tilde{G}_3^i(\tilde{x}) &= \begin{bmatrix} \tau_R \\ \tau_S \\ a_R \\ a \\ d \\ \tilde{\tau} \\ [m^R [\tau_i, m_1^s, \dots, m_5^s]]^\top \\ \ell \\ p+1 \\ 1 \end{bmatrix}, & \tilde{G}_4^i(\tilde{x}) &= \begin{bmatrix} \tau_R \\ \tau_S \\ a_R \\ a \\ c \\ \tilde{\tau} \\ [[\tau_R, m_1^s, \dots, m_5^s] m^s]^\top \\ \ell \\ p+1 \\ 0 \end{bmatrix}, \\
\tilde{G}_5^i(\tilde{x}) &= \begin{bmatrix} \tau_R \\ \tau_S \\ a_R \\ a \\ d \\ \tilde{\tau} \\ [[\tau_R, m_1^R, \dots, m_5^R] m^s]^\top \\ \ell \\ p+1 \\ 1 \end{bmatrix}, & \tilde{G}_6^i(\tilde{x}) &= \begin{bmatrix} \tau_R \\ \tau - [\mathbf{0}_{i-1}, K_{\tilde{c}}(m^R), \mathbf{0}_{n-1-i}]^\top \\ a_R \\ a + [\mathbf{0}_{i-1}, K_a(m^R, \tau_{S_i}), \mathbf{0}_{n-1-i}]^\top \\ c \\ [\tilde{\tau}_1, \dots, \tilde{\tau}_i, 3c + 3d, \tilde{\tau}_{i+2}, \dots, \tilde{\tau}_{n-1}]^\top \\ [m^R [\tau_i, m_1^R, \dots, m_5^R]]^\top \\ \ell + 1 \\ 0 \\ 0 \end{bmatrix}
\end{aligned}$$

The main idea behind the construction of the map $\tilde{G}(\tilde{x}) := \{\tilde{G}^i(\tilde{x}) : \tilde{x} \in \tilde{D}^i, i \in \mathcal{S}\}$ is to capture protocol events of the synchronization algorithm for each child node. To handle the condition where $\ell = n - 1$ such that the protocol cycles back to synchronizing the first node, we have the following

jump map for \tilde{G}_6^N ,

$$\tilde{G}_6^N(\tilde{x}) = \begin{bmatrix} \tau_R \\ \tau - [\mathbf{0}_{i-1}, K_{\tilde{o}}(\mathbf{m}^R), \mathbf{0}_{n-1-i}]^\top \\ a_R \\ a + [\mathbf{0}_{i-1}, K_a(\mathbf{m}^R, \tau_i), \mathbf{0}_{n-1-i}]^\top \\ c \\ [\tilde{\tau}_1, \dots, \tilde{\tau}_{n-2}, 3c + 3d]^\top \\ [m^R \quad [\tau_i, m_1^R, \dots, m_5^R]]^\top \\ 1 \\ 0 \\ 0 \end{bmatrix}$$

To trigger the jump map corresponding to the particular protocol event for each child node, we define the jump set as $\tilde{D} := \tilde{D}^1 \cup \tilde{D}^2 \cup \dots \cup \tilde{D}^i \cup \dots \cup \tilde{D}^N$ where $\tilde{D}^i := \tilde{D}_1^i \cup \tilde{D}_2^i \cup \tilde{D}_3^i \cup \tilde{D}_4^i \cup \tilde{D}_5^i \cup \tilde{D}_6^i$ and

$$\begin{aligned} \tilde{D}_1^i &:= \{\tilde{x} \in \tilde{\mathcal{X}} : \tau = 0, p = 0, \ell = i\}, & \tilde{D}_2^i &:= \{\tilde{x} \in \tilde{\mathcal{X}} : \tau = 0, p = 1, \ell = i\} \\ \tilde{D}_3^i &:= \{\tilde{x} \in \tilde{\mathcal{X}} : \tau = 0, p = 2, \ell = i\}, & \tilde{D}_4^i &:= \{\tilde{x} \in \tilde{\mathcal{X}} : \tau = 0, p = 3, \ell = i\} \\ \tilde{D}_5^i &:= \{\tilde{x} \in \tilde{\mathcal{X}} : \tau = 0, p = 4, \ell = i\}, & \tilde{D}_6^i &:= \{\tilde{x} \in \tilde{\mathcal{X}} : \tau = 0, \tilde{\tau}_\ell = 0, \\ & & & p = 5, \ell = i\} \end{aligned}$$

This hybrid system is denoted

$$\tilde{\mathcal{H}} = (\tilde{C}, \tilde{F}, \tilde{D}, \tilde{G}) \quad (47)$$

6.0.1 Error Model

With an abuse of notation, let $\varepsilon := (\varepsilon_1, \dots, \varepsilon_N) \in \mathbb{R}^{2(N)}$, where $\varepsilon_i = \begin{bmatrix} \tau_R - \tau_i \\ a_R - a_i \end{bmatrix}$ for each $i \in \mathcal{S}$. Then, define

$$\tilde{x}_\varepsilon := (\varepsilon, \tilde{x}) \in \tilde{\mathcal{X}}_\varepsilon := \mathbb{R}^{2(N)} \times \tilde{\mathcal{X}}$$

For each $\tilde{x}_\varepsilon \in \tilde{C}_\varepsilon := \tilde{\mathcal{X}}_\varepsilon$, the flow map is given by

$$\tilde{F}_\varepsilon(\tilde{x}_\varepsilon) = (A_F \varepsilon, \tilde{F}(\tilde{x}))$$

where

$$A_F = \begin{bmatrix} A_f & \cdots & 0 \\ \vdots & \ddots & \vdots \\ 0 & \cdots & A_f \end{bmatrix}$$

is a block diagonal matrix with N entries equal to $A_f = \begin{bmatrix} 0 & 1 \\ 0 & 0 \end{bmatrix}$.

The discrete dynamics of the protocol are modeled through the jump map $\tilde{G}_\varepsilon(\tilde{x}) := \{\tilde{G}_\varepsilon^i(\tilde{x}) : \tilde{x}_\varepsilon \in \tilde{D}_\varepsilon^i, i \in \mathcal{S}\}$ where

$$\tilde{G}_\varepsilon^i(\tilde{x}_\varepsilon) = \begin{cases} \tilde{G}_{\varepsilon_1}^i(\tilde{x}_\varepsilon) & \text{if } \tilde{x}_\varepsilon \in \tilde{D}_{\varepsilon_1}^i \setminus (\tilde{D}_{\varepsilon_2}^i \cup \tilde{D}_{\varepsilon_3}^i \cup \tilde{D}_{\varepsilon_4}^i \cup \tilde{D}_{\varepsilon_5}^i \cup \tilde{D}_{\varepsilon_6}^i) \\ \tilde{G}_{\varepsilon_2}^i(\tilde{x}_\varepsilon) & \text{if } \tilde{x}_\varepsilon \in \tilde{D}_{\varepsilon_2}^i \setminus (\tilde{D}_{\varepsilon_1}^i \cup \tilde{D}_{\varepsilon_3}^i \cup \tilde{D}_{\varepsilon_4}^i \cup \tilde{D}_{\varepsilon_5}^i \cup \tilde{D}_{\varepsilon_6}^i) \\ \tilde{G}_{\varepsilon_3}^i(\tilde{x}_\varepsilon) & \text{if } \tilde{x}_\varepsilon \in \tilde{D}_{\varepsilon_3}^i \setminus (\tilde{D}_{\varepsilon_1}^i \cup \tilde{D}_{\varepsilon_2}^i \cup \tilde{D}_{\varepsilon_4}^i \cup \tilde{D}_{\varepsilon_5}^i \cup \tilde{D}_{\varepsilon_6}^i) \\ \tilde{G}_{\varepsilon_4}^i(\tilde{x}_\varepsilon) & \text{if } \tilde{x}_\varepsilon \in \tilde{D}_{\varepsilon_4}^i \setminus (\tilde{D}_{\varepsilon_1}^i \cup \tilde{D}_{\varepsilon_2}^i \cup \tilde{D}_{\varepsilon_3}^i \cup \tilde{D}_{\varepsilon_5}^i \cup \tilde{D}_{\varepsilon_6}^i) \\ \tilde{G}_{\varepsilon_5}^i(\tilde{x}_\varepsilon) & \text{if } \tilde{x}_\varepsilon \in \tilde{D}_{\varepsilon_5}^i \setminus (\tilde{D}_{\varepsilon_1}^i \cup \tilde{D}_{\varepsilon_2}^i \cup \tilde{D}_{\varepsilon_3}^i \cup \tilde{D}_{\varepsilon_4}^i \cup \tilde{D}_{\varepsilon_6}^i) \\ \tilde{G}_{\varepsilon_6}^i(\tilde{x}_\varepsilon) & \text{if } \tilde{x}_\varepsilon \in \tilde{D}_{\varepsilon_6}^i \setminus (\tilde{D}_{\varepsilon_1}^i \cup \tilde{D}_{\varepsilon_2}^i \cup \tilde{D}_{\varepsilon_3}^i \cup \tilde{D}_{\varepsilon_4}^i \cup \tilde{D}_{\varepsilon_5}^i) \end{cases}$$

where

$$\begin{aligned} \tilde{G}_{\varepsilon_1}^i(\tilde{x}_\varepsilon) &= \begin{bmatrix} \varepsilon \\ \tilde{G}_1^i(\tilde{x}) \end{bmatrix}, \quad \tilde{G}_{\varepsilon_2}^i(\tilde{x}_\varepsilon) = \begin{bmatrix} \varepsilon \\ \tilde{G}_2^i(\tilde{x}) \end{bmatrix}, \quad \tilde{G}_{\varepsilon_3}^i(\tilde{x}_\varepsilon) = \begin{bmatrix} \varepsilon \\ \tilde{G}_3^i(\tilde{x}) \end{bmatrix}, \\ \tilde{G}_{\varepsilon_4}^i(\tilde{x}_\varepsilon) &= \begin{bmatrix} \varepsilon \\ \tilde{G}_4^i(\tilde{x}) \end{bmatrix}, \quad \tilde{G}_{\varepsilon_5}^i(\tilde{x}_\varepsilon) = \begin{bmatrix} \varepsilon \\ \tilde{G}_5^i(\tilde{x}) \end{bmatrix}, \quad \tilde{G}_{\varepsilon_6}^i(\tilde{x}_\varepsilon) = \begin{bmatrix} [\varepsilon_1, \dots, \varepsilon_i^+, \dots, \varepsilon_N]^\top \\ \tilde{G}_6^i(\tilde{x}) \end{bmatrix} \end{aligned}$$

where

$$\varepsilon_i^+ = \begin{bmatrix} \tau_R - (\tau_i - K_\sigma(\tilde{x})) \\ a_R - (a_i + K_a(\tilde{x})) \end{bmatrix}$$

These discrete dynamics apply for x in $\tilde{D}_\varepsilon := \tilde{D}_\varepsilon^1 \cup \tilde{D}_\varepsilon^2 \cup \dots \cup \tilde{D}_\varepsilon^i \cup \dots \cup \tilde{D}_\varepsilon^N$, where $\tilde{D}_\varepsilon^i := \tilde{D}_{\varepsilon_1}^i \cup \tilde{D}_{\varepsilon_2}^i \cup \tilde{D}_{\varepsilon_3}^i \cup \tilde{D}_{\varepsilon_4}^i \cup \tilde{D}_{\varepsilon_5}^i \cup \tilde{D}_{\varepsilon_6}^i$ and

$$\begin{aligned} \tilde{D}_{\varepsilon_1}^i &:= \{\tilde{x}_\varepsilon \in \tilde{\mathcal{X}}_\varepsilon : \tau = 0, p = 0, \ell = i\}, & \tilde{D}_{\varepsilon_2}^i &:= \{\tilde{x}_\varepsilon \in \tilde{\mathcal{X}}_\varepsilon : \tau = 0, p = 1, \ell = i\} \\ \tilde{D}_{\varepsilon_3}^i &:= \{\tilde{x}_\varepsilon \in \tilde{\mathcal{X}}_\varepsilon : \tau = 0, p = 2, \ell = i\}, & \tilde{D}_{\varepsilon_4}^i &:= \{\tilde{x}_\varepsilon \in \tilde{\mathcal{X}}_\varepsilon : \tau = 0, p = 3, \ell = i\} \\ \tilde{D}_{\varepsilon_5}^i &:= \{\tilde{x}_\varepsilon \in \tilde{\mathcal{X}}_\varepsilon : \tau = 0, p = 4, \ell = i\}, & \tilde{D}_{\varepsilon_6}^i &:= \{\tilde{x}_\varepsilon \in \tilde{\mathcal{X}}_\varepsilon : \tau = 0, \tilde{\tau}_\ell = 0, \\ & & & p = 5, \ell = i\} \end{aligned}$$

This hybrid system is denoted

$$\tilde{\mathcal{H}}_\varepsilon = (\tilde{C}_\varepsilon, \tilde{F}_\varepsilon, \tilde{D}_\varepsilon, \tilde{G}_\varepsilon) \quad (48)$$

and the set to render attractive for the multi-agent model is given by

$$\tilde{\mathcal{A}}_\varepsilon := \{\tilde{x}_\varepsilon \in \tilde{\mathcal{X}}_\varepsilon : \varepsilon_i = 0 \forall i \in \mathcal{S}\} \quad (49)$$

With the system defined in this manner, we certify attractivity of $\tilde{\mathcal{H}}_\varepsilon$ to $\tilde{\mathcal{A}}_\varepsilon$ through an extension of the results for the two-agent model given in Theorem 5.4. In the same order as the two-agent model, we proceed as follows:

- Define and give a result for a forward invariant set \mathcal{M} that gives the correct values of m^R and m^i such that the update laws K_{δ} and K_a give the correct values.
- Show that the forward invariant set \mathcal{M} is finite time attractive.
- Utilizing the same Lyapunov-based approach for the two-agent system, a function $\tilde{V} : \tilde{\mathcal{X}}_{\varepsilon} \rightarrow \mathbb{R}_{\geq 0}$ is defined as an extension of the function given in (28).
- Infinitesimal properties of \tilde{V} are established across flows and jumps of the system $\tilde{\mathcal{H}}_{\varepsilon}$ via separate lemmas.

Following these results, the main result is presented showing attractivity of the set of interest. To demonstrate the feasibility of the algorithm, a numerical example featuring a three-agent system illustrating the convergence properties of $\tilde{\mathcal{H}}_{\varepsilon}$ is simulated.

6.0.2 Properties of the Multi-agent model

Given that the multi-agent model is an extension of the two-agent model, we remind the reader that the accuracy of the update laws K_{δ} and K_a given in (18) and (19) depend on the assigned values of the memory buffers, namely m^R and m^i for the multi-agent model. Therefore, to facilitate the analysis of $\tilde{\mathcal{H}}_{\varepsilon}$ in rendering the set $\mathcal{A}_{\varepsilon}$ asymptotically attractive, we define a new set modified from the set \mathcal{M} given in (25) that gives the state space of values of m^R and m^i for which the update laws K_{δ} and K_a give the correct values. In particular, consider the set

$$\mathcal{M} := \mathcal{M}_1 \cup \mathcal{M}_2 \cup \mathcal{M}_3 \cup \mathcal{M}_4 \cup \mathcal{M}_5 \cup \mathcal{M}_6 \quad (50)$$

where

$$\begin{aligned}
\mathcal{M}_1 &:= \{\tilde{x}_\varepsilon \in \mathcal{X}_\varepsilon : p=0, q=0\} \\
\mathcal{M}_2 &:= \{\tilde{x}_\varepsilon \in \mathcal{X}_\varepsilon : p=1, q=1, m_1^R - \rho_R(\tilde{x}_\varepsilon, 0) = 0\} \\
\mathcal{M}_3 &:= \{\tilde{x}_\varepsilon \in \mathcal{X}_\varepsilon : p=2, q=0, m_1^i - \rho_i(\tilde{x}_\varepsilon, 0) = 0, \\
&\quad m_2^i - \rho_R(\tilde{x}_\varepsilon, d) = 0\} \\
\mathcal{M}_4 &:= \{\tilde{x}_\varepsilon \in \mathcal{X}_\varepsilon : p=3, q=1, m_1^i - \rho_i(\tilde{x}_\varepsilon, 0) = 0, \\
&\quad m_2^i - \rho_i(\tilde{x}_\varepsilon, d) = 0, m_3^i - \rho_R(\tilde{x}_\varepsilon, c+d) = 0\} \\
\mathcal{M}_5 &:= \{\tilde{x}_\varepsilon \in \mathcal{X}_\varepsilon : p=4, q=0, m_1^R - \rho_R(\tilde{x}_\varepsilon, 0) = 0, \\
&\quad m_2^R - \rho_i(\tilde{x}_\varepsilon, d) = 0, m_3^R - \rho_i(\tilde{x}_\varepsilon, c+d) = 0, \\
&\quad m_4^R - \rho_R(\tilde{x}_\varepsilon, 2d+c) = 0\} \\
\mathcal{M}_6 &:= \{\tilde{x}_\varepsilon \in \mathcal{X}_\varepsilon : p=5, q=1, m_1^R - \rho_R(\tilde{x}_\varepsilon, 0) = 0, \\
&\quad m_2^R - \rho_R(\tilde{x}_\varepsilon, c) = 0, m_3^R - \rho_i(\tilde{x}_\varepsilon, c+d) = 0, \\
&\quad m_4^R - \rho_i(\tilde{x}_\varepsilon, 2c+d) = 0, m_5^R - \rho_R(\tilde{x}_\varepsilon, 2c+2d) = 0\}
\end{aligned}$$

and

$$\begin{aligned}
\rho_R(\tilde{x}_\varepsilon, \beta) &= \left(\tau_R - a_R(((1-q)c+qd) - \tau) \right) - a_R(\beta) \\
\rho_i(\tilde{x}_\varepsilon, \beta) &= \left(\tau_i - a_i(((1-q)c+qd) - \tau) \right) - a_i(\beta)
\end{aligned} \tag{51}$$

for some $\beta > 0$, i.e., $\beta = 0, c + d, 2c + d, 2c + 2d$.

Lemma 6.1. *The set \mathcal{M} is forward invariant for the hybrid system $\tilde{\mathcal{H}}_\varepsilon$.*

Proof. This result follows from the proof of Lemma 4.3 since the variables τ, p, q, m^R , and m^i have identical dynamics to the corresponding variables in the two-agent model. \square

Lemma 6.2. *Let constants $d \geq c > 0$ be given. For each maximal solution ϕ to $\tilde{\mathcal{H}}_\varepsilon$, there exists a $T^* \geq 0$ such that for any $(t, j) \in \text{dom } \phi$ with $t+j \geq T^*$, $\phi(t, j) \in \mathcal{M}$.*

Proof. Pick a solution ϕ with initial condition $\phi(0, 0) \in C_\varepsilon \cup \tilde{D}_\varepsilon$. From the initial condition, the solution flows and jumps according to the dynamics of \mathcal{H} . Observe that when $\phi \in C_\varepsilon$, $\dot{p} = 0$ and when $\phi \in \tilde{D}_\varepsilon$, $p^+ = p + 1$ following jumps according to $G_{\varepsilon_\ell}^i(\tilde{x}_\varepsilon)$, $\ell \in \{1, 2, 3, 4, 5\}$. However, for jumps according to $G_{\varepsilon_6}^i(\tilde{x}_\varepsilon)$, $p^+ = 0$ then by also noting that $q^+ = 0$,

$G_{\varepsilon_6}^i(\tilde{x}_\varepsilon) \subset \mathcal{M}_6$. Therefore, due to the monotonic behavior of p following jumps according to $G_{\varepsilon_\ell}^i(\tilde{x}_\varepsilon)$, $\ell \in \{1, 2, 3, 4, 5\}$, at $t + j \geq T^*$ the solution jumps according to $G_{\varepsilon_6}^i(\tilde{x}_\varepsilon)$, then following the notions on forward invariance for \mathcal{M} in Lemma 6.1, the solution remains in \mathcal{M} as $t + j \rightarrow \infty$. \square

6.0.3 Results

To show attractivity of $\tilde{\mathcal{A}}_\varepsilon$ in (49) for $\tilde{\mathcal{H}}_\varepsilon$ in (48), we utilize a similar Lyapunov-based approach to the two-node model as presented in (12). Define the function $\tilde{V} : \tilde{\mathcal{X}}_\varepsilon \rightarrow \mathbb{R}_{\geq 0}$ as

$$\begin{aligned} \tilde{V}(\tilde{x}_\varepsilon) &= \varepsilon_1^\top \exp(A_f^\top \tilde{\tau}_1) P \exp(A_f \tilde{\tau}_1) \varepsilon_1 + \dots + \varepsilon_i^\top \exp(A_f^\top \tilde{\tau}_i) P \exp(A_f \tilde{\tau}_i) \varepsilon_i + \dots \\ &\quad + \varepsilon_N^\top \exp(A_f^\top \tilde{\tau}_N) P \exp(A_f \tilde{\tau}_N) \varepsilon_N \\ &= \varepsilon^\top Q(\tilde{\tau})^\top \mathcal{P} Q(\tilde{\tau}) \varepsilon \end{aligned} \tag{52}$$

defined for each $\tilde{x}_\varepsilon \in C_\varepsilon \cup \tilde{D}_\varepsilon$ where $Q(\tau_{\mathcal{H}}) = \text{diag}(\exp(A_F \tau_{\mathcal{H}_1}), \dots, \exp(A_F \tau_{\mathcal{H}_N}))$ and $\mathcal{P} = \text{diag}(P, \dots, P)$ where $P \succ 0$. Furthermore, note the existence of two positive scalars α_1 and α_2 such that

$$\alpha_1 |\tilde{x}_\varepsilon|_{\tilde{\mathcal{A}}_\varepsilon}^2 \leq V(\tilde{x}_\varepsilon) \leq \alpha_2 |\tilde{x}_\varepsilon|_{\tilde{\mathcal{A}}_\varepsilon}^2 \tag{53}$$

The function \tilde{V} satisfies the following infinitesimal properties.

Lemma 6.3. *Let the hybrid system $\tilde{\mathcal{H}}_\varepsilon$ with constants $d \geq c > 0$ be given. For each $\tilde{x}_\varepsilon \in \tilde{C}$,*

$$\langle \nabla V(\tilde{x}_\varepsilon), \tilde{F}_\varepsilon(\tilde{x}_\varepsilon) \rangle = 0$$

Proof. This result follows through direct calculation of $\langle \nabla V(\tilde{x}_\varepsilon), \tilde{F}_\varepsilon(\tilde{x}_\varepsilon) \rangle$. \square

Lemma 6.4. *Let the hybrid system $\tilde{\mathcal{H}}_\varepsilon$ with constants $d \geq c > 0$ be given. If there exist a constant $\mu > 0$ and a positive definite symmetric matrix P such that*

$$A_g^\top \exp((3c + 3d)A_f^\top) P \exp((3c + 3d)A_f) A_g - P \prec 0 \tag{54}$$

is satisfied where $A_g = \begin{bmatrix} 0 & \gamma_1 \\ 0 & 1 - \mu\gamma_2 \end{bmatrix}$ with $\gamma_1 = \frac{3c+4d}{2}$ and $\gamma_2 = 2c + 2d$, then for each $\tilde{x}_\varepsilon \in \mathcal{M} \cap \tilde{D}_\varepsilon$

$$V(g) - V(\tilde{x}_\varepsilon) \leq \begin{cases} 0 & \text{if } g \in \tilde{G}_\varepsilon(\tilde{x}_\varepsilon) \setminus \tilde{G}_6^i(\tilde{x}_\varepsilon), i \in \mathcal{V} \\ -\sigma \varepsilon_i^\top \varepsilon_i & \text{if } g \in \tilde{G}_6^i(\tilde{x}_\varepsilon), i \in \mathcal{V} \end{cases} \tag{55}$$

where

$$\sigma \in \left(0, \lambda_{\min} \left(A_g^\top \exp \left((3c + 3d)A_f^\top \right) P \exp \left((3c + 3d)A_f \right) A_g - P \prec 0 \right) \right)$$

Proof. Consider the Lyapunov function candidate $\tilde{V} : \tilde{\mathcal{X}}_\varepsilon \rightarrow \mathbb{R}_{\geq 0}$ in (52). For each $\tilde{x}_\varepsilon \in \tilde{D}_\varepsilon \setminus \tilde{D}_{\varepsilon_6}^i$, $i \in \mathcal{V}$ and each $g \in \tilde{G}_\varepsilon(\tilde{x}_\varepsilon) \setminus \tilde{G}_6^i(\tilde{x}_\varepsilon)$, $i \in \mathcal{V}$, we have that $V(g) - V(\tilde{x}_\varepsilon) = 0$. Now for each $\tilde{x}_\varepsilon \in \tilde{D}_{\varepsilon_6}^i \cap \mathcal{M}_6$, $i \in \mathcal{V}$ we have that $\tilde{\tau}_i = 0$ then for each $g \in \tilde{G}_6^i(\tilde{x}_\varepsilon)$, $i \in \mathcal{V}$,

$$\begin{aligned} V(\tilde{G}_{\varepsilon_6}^i(\tilde{x}_\varepsilon)) - V(\tilde{x}_\varepsilon) &= \\ & \left[\varepsilon_i + \begin{bmatrix} -K_{\tilde{\delta}}(\tilde{x}_\varepsilon) \\ K_a(\tilde{x}_\varepsilon) \end{bmatrix} \right]^\top \exp \left((3c + 3d)A_f^\top \right) P \exp \left((3c + 3d)A_f \right) \left[\varepsilon_i + \begin{bmatrix} -K_{\tilde{\delta}}(\tilde{x}_\varepsilon) \\ K_a(\tilde{x}_\varepsilon) \end{bmatrix} \right] \\ & \quad - \varepsilon_i^\top \exp \left((0)A_f^\top \right) P \left((0)A_f \right) \varepsilon_i \\ &= \left[\varepsilon_i + \begin{bmatrix} -K_{\tilde{\delta}}(\tilde{x}_\varepsilon) \\ K_a(\tilde{x}_\varepsilon) \end{bmatrix} \right]^\top \exp \left((3c + 3d)A_f^\top \right) P \exp \left((3c + 3d)A_f \right) \left[\varepsilon_i + \begin{bmatrix} -K_{\tilde{\delta}}(\tilde{x}_\varepsilon) \\ K_a(\tilde{x}_\varepsilon) \end{bmatrix} \right] \\ & \quad - \varepsilon_i^\top P \varepsilon_i \end{aligned}$$

Recall from the proof of Lemma 5.2, that for jumps with reset $g = \tilde{G}_{\varepsilon_6}^i(x)$ for $x_\varepsilon \in \mathcal{M}$, the corrections $K_{\tilde{\delta}}(p, m)$, $K_a(m, \tau_k)$ applied to τ_i , a_i , respectively, give $K_{\tilde{\delta}}(\tilde{x}_\varepsilon) = -\varepsilon_\tau + \gamma_1 \varepsilon_a$ and $K_a(\tilde{x}_\varepsilon) = \mu \gamma_2 \varepsilon_a$ where $\gamma_1 = \frac{(3c+4d)}{2}$ and

$\gamma_2 = 2c + 2d$. One then has,

$$\begin{aligned}
V(\tilde{G}_{\varepsilon_6}^i(\tilde{x}_\varepsilon)) - V(\tilde{x}_\varepsilon) &= \left[\varepsilon_i + \begin{bmatrix} -K_{\tilde{\delta}}(\tilde{x}_\varepsilon) \\ K_a(\tilde{x}_\varepsilon) \end{bmatrix} \right]^\top \exp((3c + 3d)A_f^\top) P \exp((3c + 3d)A_f) \left[\varepsilon_i + \begin{bmatrix} -K_{\tilde{\delta}}(\tilde{x}_\varepsilon) \\ K_a(\tilde{x}_\varepsilon) \end{bmatrix} \right] \\
&\quad - \varepsilon_i^\top P \varepsilon_i \\
&= \begin{bmatrix} \varepsilon_{\tau_i} - \varepsilon_{\tau_i} + \gamma_1 \varepsilon_{a_i} \\ \varepsilon_{a_i} - \mu \gamma_2 \varepsilon_{a_i} \end{bmatrix}^\top \exp((3c + 3d)A_f^\top) P \exp((3c + 3d)A_f) \begin{bmatrix} \varepsilon_{\tau_i} - \varepsilon_{\tau_i} + \gamma_1 \varepsilon_{a_i} \\ \varepsilon_{a_i} - \mu \gamma_2 \varepsilon_{a_i} \end{bmatrix} \\
&\quad - \varepsilon_i^\top P \varepsilon_i \\
&= \left[I \varepsilon_i + \begin{bmatrix} -1 & \gamma_1 \\ 0 & -\mu \gamma_2 \end{bmatrix} \varepsilon_i \right]^\top \exp((3c + 3d)A_f^\top) P \exp((3c + 3d)A_f) \left[I \varepsilon_i + \begin{bmatrix} -1 & \gamma_1 \\ 0 & -\mu \gamma_2 \end{bmatrix} \varepsilon_i \right] \\
&\quad - \varepsilon_i^\top P \varepsilon_i \\
&= \left[\left(I + \begin{bmatrix} -1 & \gamma_1 \\ 0 & -\mu \gamma_2 \end{bmatrix} \right) \varepsilon_i \right]^\top \exp((3c + 3d)A_f^\top) P \exp((3c + 3d)A_f) \left[\left(I + \begin{bmatrix} -1 & \gamma_1 \\ 0 & -\mu \gamma_2 \end{bmatrix} \right) \varepsilon_i \right] \\
&\quad - \varepsilon_i^\top P \varepsilon_i \\
&= \varepsilon_i \begin{bmatrix} 0 & \gamma_1 \\ 0 & 1 - \mu \gamma_2 \end{bmatrix}^\top \exp((3c + 3d)A_f^\top) P \exp((3c + 3d)A_f) \begin{bmatrix} 0 & \gamma_1 \\ 0 & 1 - \mu \gamma_2 \end{bmatrix} \varepsilon_i \\
&\quad - \varepsilon_i^\top P \varepsilon_i \\
&= \varepsilon_i^\top A_g^\top \exp((3c + 3d)A_f^\top) P \exp((3c + 3d)A_f) A_g \varepsilon_i - \varepsilon_i^\top P \varepsilon_i \\
&= \varepsilon_i^\top \left(A_g^\top \exp((3c + 3d)A_f^\top) P \exp((3c + 3d)A_f) A_g - P \right) \varepsilon_i
\end{aligned}$$

where $A_g = \begin{bmatrix} 0 & \gamma_1 \\ 0 & 1 - \mu \gamma_2 \end{bmatrix}$. Then, by continuity of condition (57),

$$V(\tilde{G}_{\varepsilon_6}^i) - V(\tilde{x}_\varepsilon) \leq -\sigma \varepsilon_i^\top \varepsilon_i \quad (56)$$

where

$$\sigma \in \left(0, \lambda_{\min} \left(A_g^\top \exp((3c + 3d)A_f^\top) P \exp((3c + 3d)A_f) A_g - P \prec 0 \right) \right)$$

□

Theorem 6.5. *Let the hybrid system $\tilde{\mathcal{H}}_\varepsilon$ with constants $d \geq c > 0$ be given. If there exist a constant $\mu > 0$ and positive definite symmetric matrix P such that*

$$A_g^\top \exp((3c + 3d)A_f^\top) P \exp((3c + 3d)A_f) A_g - P \prec 0 \quad (57)$$

is satisfied where $A_g = \begin{bmatrix} 0 & \gamma_1 \\ 0 & 1-\mu\gamma_2 \end{bmatrix}$ with $\gamma_1 = \frac{3c+4d}{2}$ and $\gamma_2 = 2c + 2d$, then $\tilde{\mathcal{A}}_\varepsilon$ is globally attractive for $\tilde{\mathcal{H}}_\varepsilon$.

Proof. Pick a maximal solution $\phi \in \mathcal{S}_{\tilde{\mathcal{H}}_\varepsilon}$ with initial condition $\phi \in (\tilde{C}_\varepsilon \cup \tilde{D}_\varepsilon) \cap \mathcal{M}$ and consider the function V in (52). Recall the dynamics of V from Lemmas 6.3 and 6.4 for $\tilde{x}_\varepsilon \in \tilde{C}_\varepsilon \cup \tilde{D}_\varepsilon$,

$$\langle \nabla \tilde{V}(\tilde{x}_\varepsilon), \tilde{F}_\varepsilon(\tilde{x}_\varepsilon) \rangle = 0$$

and

$$\tilde{V}(g) - \tilde{V}(\tilde{x}_\varepsilon) \leq \begin{cases} 0 & \text{if } g \in \tilde{G}_\varepsilon(\tilde{x}_\varepsilon) \setminus \tilde{G}_6^i(\tilde{x}_\varepsilon), i \in \mathcal{V} \\ -\sigma_i \varepsilon_i^\top \varepsilon_i & \text{if } g = \tilde{G}_6^i(\tilde{x}_\varepsilon), i \in \mathcal{V} \end{cases}$$

Observe that V remains constant during flows and following any jump $g \in \tilde{G}_\varepsilon(\tilde{x}_\varepsilon) \setminus \tilde{G}_6^i(\tilde{x}_\varepsilon), i \in \mathcal{V}$. It is only following jumps according to $g = \tilde{G}_6^i(\tilde{x}_\varepsilon), i \in \mathcal{V}$ that V observes a decrease.

Now, by noting the dynamics of the variable s , namely that it increments by one following each jump $g = \tilde{G}_6^i(\tilde{x}_\varepsilon), i \in \mathcal{V} \setminus \{n-1\}$ and resets to one following a jump according to $g = \tilde{G}_6^{n-1}(\tilde{x}_\varepsilon)$, we have that the trajectory of ϕ_s is cyclic. Moreover, we have that the algorithm iterates through each node $i \in \mathcal{V}$ applying the corrections $K_{\tilde{o}}(p, m)$, $K_a(m, \tau_k)$ to ε_i . Therefore, due to the deterministic nature of the timers τ^* and $\tilde{\tau}$ that govern the flow and jumps of the system, there exists a hybrid time (t, j) such that $t + j \geq T^* \geq 0$ where the algorithm has applied the corrections $K_{\tilde{o}}(p, m)$, $K_a(m, \tau_k)$ to ε_i for each $i \in \mathcal{V}$. Then we have that

$$V(\phi(t, j)) = - \sum_{i=1}^{n-1} \sigma_i \varepsilon_i^\top(t^i, j^i) \varepsilon_i(t^i, j^i) \quad \forall (t, j) \in \{\text{dom } \phi : t + j \geq T^*\}$$

where $(t^i, j^i) \in \{\text{dom } \phi : \phi(t, j) \in \tilde{D}_{\varepsilon_6}^i, i \in \mathcal{V}\}$ denotes the time at which the corrections $K_{\tilde{o}}(p, m)$, $K_a(m, \tau_k)$ are applied to ε_i . Then, taking the limit of $V(\phi(t, j))$ we have that

$$\lim_{t+j \rightarrow \infty} V(\phi(t, j)) = 0$$

allowing us to conclude attractivity to the set $\tilde{\mathcal{A}}_\varepsilon$ for $\tilde{\mathcal{H}}_\varepsilon$ and complete the proof. \square

7 Numerical Results

7.1 Two-agent system

7.1.1 Nominal Setting

In this first example, we present a numerical simulation of the two-agent system for the nominal setting that validates our theoretical results, namely we show that with the conditions in (38) satisfied, the trajectories of the simulation converge to the desired set.

Example 7.1. Consider Nodes i and k with dynamics as in (1) with data $a_i = 1$, $a_k = 1.8$ and $c = 0.1$, $d = 0.2$ to the system \mathcal{H} . Setting $\mu = 0.833$, condition (38) is satisfied with $P = \begin{bmatrix} 6.2594 & -0.5219 \\ -0.5219 & 11.4302 \end{bmatrix}$. Simulating the system, Figure 5 shows the trajectories of the error in the clocks and error in the clock rates of Nodes i and k for a solution ϕ to the system such that $\phi(0,0) \in (C \cup D) \cap \mathcal{M}$. Figure 5 also shows the plot of V evaluated along the solution. Notice, that V converges to zero asymptotically following several periodic executions of the algorithm. Observe that the behavior of clock error is more stable than the conventional sender-receiver algorithm simulated in Figure 3.⁶

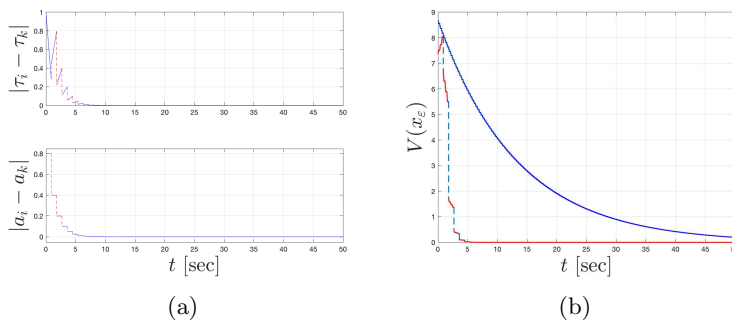


Figure 5: Figure 5(a) gives the evolution of the error in the clocks and clock rates of Nodes i and k . Figure 5(b) gives V evaluated along the solution.

7.1.2 Variable propagation delay due to communication noise

In the next example, we simulate the case of noise in the communication channel that contributes to a variable propagation delay d . Noise in the

⁶Code at github.com/HybridSystemsLab/HybridSenRecClockSync

communication channel makes the propagation delay between nodes i and k no longer symmetric.

Example 7.2. Consider the same clock dynamics from the previous example, i.e., $a_i = 1.1$, $a_k = 0.75$, with $\mu = 0.3571$ and condition (38) satisfied for $c = 0.2$, $d = 0.5$, and $P = \begin{bmatrix} 5.435 & 1.041 \\ 1.041 & 16.0982 \end{bmatrix}$. Now, with $[d_1, d_2]$ defining the allowed values of d with $d_1 = 0.49$ and $d_2 = 0.51$, we generate variable propagation delay by replacing the dynamics of τ in (13) by

$$\begin{aligned} \dot{\tau} &= -1 & \tau &\in [0, d_2] \\ \tau^+ &\in \cup_{d \in [d_1, d_2]} (1 - q)d + qc & \tau &= 0 \end{aligned}$$

Figure 8 shows a simulation of the trajectories of the error in the clocks and error in the clock rates of Nodes i and k . Observe that absolute error in the clocks converges to zero even in the presence of the perturbation after several periodic executions of the algorithm. The error in clock rates is also able to converge sufficiently close to zero but suffers from some observed variability due to the noise.⁷

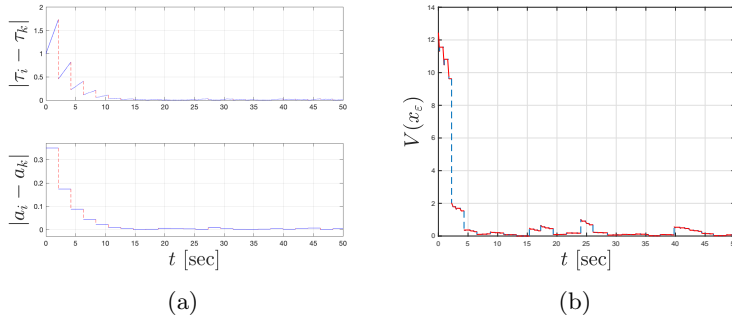


Figure 6: Figure 5(a) gives the evolution of the error in the clocks and clock rates of Nodes i and k subject to noise on the communication channel. Figure 5(b) gives V evaluated along the solution.

7.1.3 Time-varying clock rates

In the next example, we consider the common scenario of time-varying clock skews at both nodes i and k . This noise is injected at the clock dynamics $\dot{\tau}_i$ and $\dot{\tau}_k$. The system is then simulated with the remaining dynamics left unchanged.

⁷Code at github.com/HybridSystemsLab/HybridSenRecClockSync

Example 7.3. For $c = 0.2$ and $d = 0.5$, consider nodes i and k with clock dynamics

$$\begin{aligned}\dot{\tau}_i &= a_i + m_a \\ \dot{\tau}_k &= a_k + m_a\end{aligned}$$

where $a_i = 1.1$, $a_k = 0.75$, and $m_a \in (-0.3, 0.3)$ is a Gaussian injected noise on the clock dynamics. Letting $\mu = 0.3571$, condition (38) is satisfied with $P = \begin{bmatrix} 5.435 & 1.041 \\ 1.041 & 16.0982 \end{bmatrix}$. Simulating the system, Figure 7 shows the trajectories of the error in the clocks and error in the clock rates of Nodes i and k . Again, the system is able to converge after a couple of executions of the algorithm. The error on the clocks observes the most variability due to simulated noise.⁸

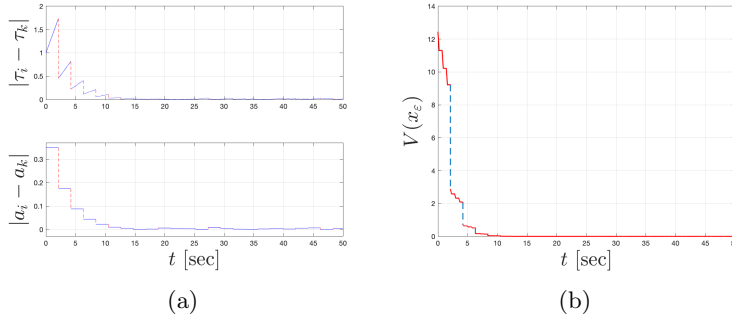


Figure 7: Figure 5(a) gives the evolution of the error in the clocks and clock rates of Nodes i and k subject to noise m_a on the clock dynamics. Figure 5(b) gives V evaluated along the solution.

7.2 Multi-agent model

In this section we present numerical results for the multi-agent model to validate our theoretical results and draw comparisons with other multi-agent clock synchronization models from the literature.

Example 7.4. Consider a network of three nodes $\{R, 1, 2\}$ where R denotes the reference or parent node while nodes 1 and 2 denote the synchronizing child nodes. The data of this system is given by $a_R, a_1, a_2 \in [0.5, 1.5]$ and $c = 0.1$, $d = 0.2$ with $\mu = 0.833$. Simulating the multi-agent system $\tilde{\mathcal{H}}$,

⁸Code at github.com/HybridSystemsLab/HybridSenRecClockSync

Figure 7(a) shows the trajectories of the error in the clocks and error in the clock rates of Nodes 1 and 2 with respect to Node R . Note that the errors with respect to each clock converge after several executions of the algorithm on the respective clocks at Nodes 1 and 2.⁹

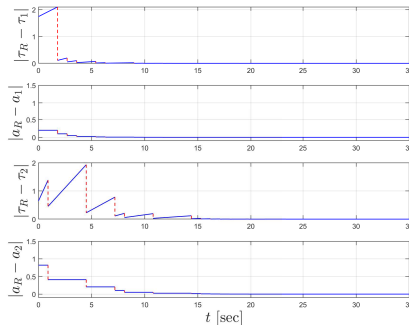


Figure 8: The evolution of the error in the clocks and clock rates of Nodes 1 and 2 with respect to Node R .

8 Conclusion

In this paper, we introduced a sender-receiver clock synchronization algorithm with sufficient design conditions ensuring synchronization. Results were given to show asymptotic attractivity of a set of interest reflecting the desired synchronized setting. Numerical results validating the attractivity of the system to the set of interest were also given. An additional model to capture the multi-agent setting was presented with a numerical example to demonstrate its feasibility. In future work we will study stability of the system and robustness properties to specific perturbations.

References

- [1] S. Samii, H. Zinner, Level 5 by layer 2: Time-sensitive networking for autonomous vehicles, *IEEE Communications Standards Magazine* 2 (2) (2018) 62–68.
- [2] J. C. Eidson, Measurement, control, and communication using IEEE 1588, Springer Science & Business Media, 2006.

⁹Code at github.com/HybridSystemsLab/HybridSenRecMultiClockSync

- [3] S. Graham, P. R. Kumar, Time in general-purpose control systems: the control time protocol and an experimental evaluation, in: 2004 43rd IEEE Conference on Decision and Control (CDC) (IEEE Cat. No.04CH37601), Vol. 4, 2004, pp. 4004–4009 Vol.4. doi:10.1109/CDC.2004.1429378.
- [4] W. Zhang, M. S. Branicky, S. M. Phillips, Stability of networked control systems, *IEEE Control Systems Magazine* 21 (1) (2001) 84–99. doi:10.1109/37.898794.
- [5] J. Nilsson, Real-time control systems with delays, Ph.D. thesis, Lund University (1998).
- [6] J. P. Hespanha, P. Naghshtabrizi, Y. Xu, A survey of recent results in networked control systems, *Proceedings of the IEEE* 95 (1) (2007) 138–162.
- [7] Y.-C. Wu, Q. Chaudhari, E. Serpedin, Clock synchronization of wireless sensor networks, *IEEE Signal Processing Magazine* 28 (1) (2010) 124–138.
- [8] B. Sundararaman, U. Buy, A. D. Kshemkalyani, Clock synchronization for wireless sensor networks: a survey, *Ad hoc networks* 3 (3) (2005) 281–323.
- [9] O. Simeone, U. Spagnolini, Y. Bar-Ness, S. H. Strogatz, Distributed synchronization in wireless networks, *IEEE Signal Processing Magazine* 25 (5) (2008) 81–97.
- [10] S. M. LaValle, M. B. Egerstedt, On time: Clocks, chronometers, and open-loop control, in: 2007 46th IEEE Conference on Decision and Control, IEEE, 2007, pp. 1916–1922.
- [11] M. Guarro, F. Ferrante, R. Sanfelice, State estimation of linear systems over a network subject to sporadic measurements, delays, and clock mismatches, *IFAC-PapersOnLine* 51 (23) (2018) 313–318.
- [12] Y. Nakamura, K. Hirata, K. Sugimoto, Synchronization of multiple plants over networks via switching observer with time-stamp information, in: 2008 SICE Annual Conference, IEEE, 2008, pp. 2859–2864.
- [13] D. L. Mills, Internet time synchronization: the network time protocol, *IEEE Transactions on communications* 39 (10) (1991) 1482–1493.

- [14] IEEE, IEEE standard for a precision clock synchronization protocol for networked measurement and control systems, IEEE Std 1588-2008 (Revision of IEEE Std 1588-2002) (2008) 1–300.
- [15] S. Ganeriwal, R. Kumar, M. B. Srivastava, Timing-sync protocol for sensor networks, in: Proceedings of the 1st international conference on Embedded networked sensor systems, ACM, 2003, pp. 138–149.
- [16] N. M. Freris, S. R. Graham, P. Kumar, Fundamental limits on synchronizing clocks over networks, IEEE Transactions on Automatic Control 56 (6) (2010) 1352–1364.
- [17] L. Schenato, F. Fiorentin, Average timesynch: A consensus-based protocol for clock synchronization in wireless sensor networks, Automatica 47 (9) (2011) 1878–1886.
- [18] R. Carli, S. Zampieri, Network clock synchronization based on the second-order linear consensus algorithm, IEEE Transactions on Automatic Control 59 (2) (2014) 409–422. doi:10.1109/TAC.2013.2283742.
- [19] S. Bolognani, R. Carli, E. Lovisari, S. Zampieri, A randomized linear algorithm for clock synchronization in multi-agent systems, IEEE Transactions on Automatic Control 61 (7) (2015) 1711–1726.
- [20] E. Garone, A. Gasparri, F. Lamonaca, Clock synchronization protocol for wireless sensor networks with bounded communication delays, Automatica 59 (2015) 60–72.
- [21] M. Guarro, R. G. Sanfelice, Hyntp: A distributed hybrid algorithm for time synchronization, arXiv preprint arXiv:2105.00165.
- [22] R. Goebel, R. G. Sanfelice, A. R. Teel, Hybrid Dynamical Systems: Modeling, Stability, and Robustness, Princeton University Press, 2012.
- [23] M. Guarro, R. Sanfelice, An adaptive hybrid control algorithm for sender-receiver clock synchronization, IFAC-PapersOnLine 53 (2) (2020) 1906–1911.
- [24] N. M. Freris, V. S. Borkar, P. Kumar, A model-based approach to clock synchronization, in: Proceedings of the 48h IEEE Conference on Decision and Control (CDC) held jointly with 2009 28th Chinese Control Conference, IEEE, 2009, pp. 5744–5749.

- [25] F. Ferrante, F. Gouaisbaut, R. G. Sanfelice, S. Tarbouriech, State estimation of linear systems in the presence of sporadic measurements, *Automatica* 73 (2016) 101 – 109.
- [26] R. G. Sanfelice, R. Goebel, A. R. Teel, Invariance principles for hybrid systems with connections to detectability and asymptotic stability, *IEEE Transactions on Automatic Control* 52 (12) (2007) 2282–2297. doi:10.1109/TAC.2007.910684.
- [27] D. Macii, D. Fontanelli, D. Petri, A master-slave synchronization model for enhanced servo clock design, in: *2009 International Symposium on Precision Clock Synchronization for Measurement, Control and Communication*, 2009, pp. 1–6. doi:10.1109/ISPCS.2009.5340199.
- [28] M. Guarro, R. G. Sanfelice, HyNTP: An adaptive hybrid network time protocol for clock synchronization in heterogeneous distributed systems, in: *2020 American Control Conference (ACC)*, 2020, pp. 1025–1030. doi:10.23919/ACC45564.2020.9147245.